Erskine Sandstone Formation: A provenance and geochronological study within the Fitzroy Trough, Western Australia

Thesis submitted in accordance with the requirements of the University of Adelaide for an Honours Degree in Geology

Michael C. Thomas

November 2012

THE UNIVERSITY of ADELAIDE

ERSKINE SANDSTONE FORMATION: A PROVENANCE AND GEOCHRONOLOGICAL STUDY WITHIN THE FITZROY TROUGH, WESTERN AUSTRALIA

PROVENANCE OF THE ERSKINE SANDSTONE FORMATION

ABSTRACT

The Erskine Sandstone Formation is located in the Fitzroy Trough, within the northern Canning Basin, Western Australia. The provenance evolution of the onshore Triassic sandstone of the Erskine Sandstone Formation has not previously been researched. Field work was conducted predominantly at two areas, the Erskine Range, the type section of the Sandstone, and the May River outcrops which include the Pinnacle Rock outcrop. Field work in the area showed a transitional boundary between the underlying Blina Shale and the Erskine Sandstone Formation making identification of the boundary zones difficult.

Through the use of U-Pb zircon analysis on samples taken from the Erskine Range and the May River, this study suggests the two outcrops have differing sources. Samples taken from the Erskine Range contain Permian aged sediments which are not present in the May River samples. The significant presence of Mesoproterozoic sediments in the May River samples which are not reflected in the Erskine Range samples further suggests different sources. The large presence of Palaeoproterozoic sediments in both the Erskine Range and the May River outcrops suggests the uranium rich King Leopold Ranges is a possible source. These sediments, combined with the presence of reductants in the Erskine Sandstone Formation suggest the possibility of sandstone-hosted uranium mineralisation within the Fitzroy Trough. Other possible sediment sources include the Musgrave Block and Arunta Inlier, located to the south, and suggest a complex detrital history of the Fitzroy Trough.

KEYWORDS

Erskine Sandstone Formation; Fitzroy Trough; Canning Basin; Western Australia;

geochronology; zircon; Triassic; Uranium.

TABLE OF CONTENTS

LIST OF TABLES AND FIGURES

INTRODUCTION

The Triassic Erskine Sandstone Formation is the onshore equivalent of the vast gas reservoir rocks of the offshore Canning Basin (Longley *et al.* 2004) and is also highly prospective for uranium. Despite this, very little is known about its provenance, or the provenance of the underlying Palaeozoic of the 18 km thick Canning Basin succession (Yeates *et al.* 1984, Cadman *et al.* 1993). Several models have previously been proposed, with one such model suggesting the Erskine Sandstone formed by detrital deposition of sediments derived from the unroofing of the uranium rich King Leopold Ranges (McKay & Miezitis 2001). Another model suggests that sediments were derived from the south, due to the presence of northerly current directions in the Erskine Sandstone Formation, indicating a source area south of the Fitzroy Trough (Towner 1981).

The Erskine Sandstone Formation is situated within the Fitzroy Trough, a sub-basin of the north Canning Basin, northern Western Australia (Figure 1)(Cadman *et al.* 1993). Sediments in the Canning Basin range in age from Ordovician to Quaternary (Yeates *et al.* 1984, Cadman *et al.* 1993), with the Erskine Sandstone Formation associated with marine regression during the Middle Triassic (Cadman *et al.* 1993). There has also been some conjecture as to whether the sparse outcrop along the May River correlates with the type-section located within the Erskine Range (Figure 2).

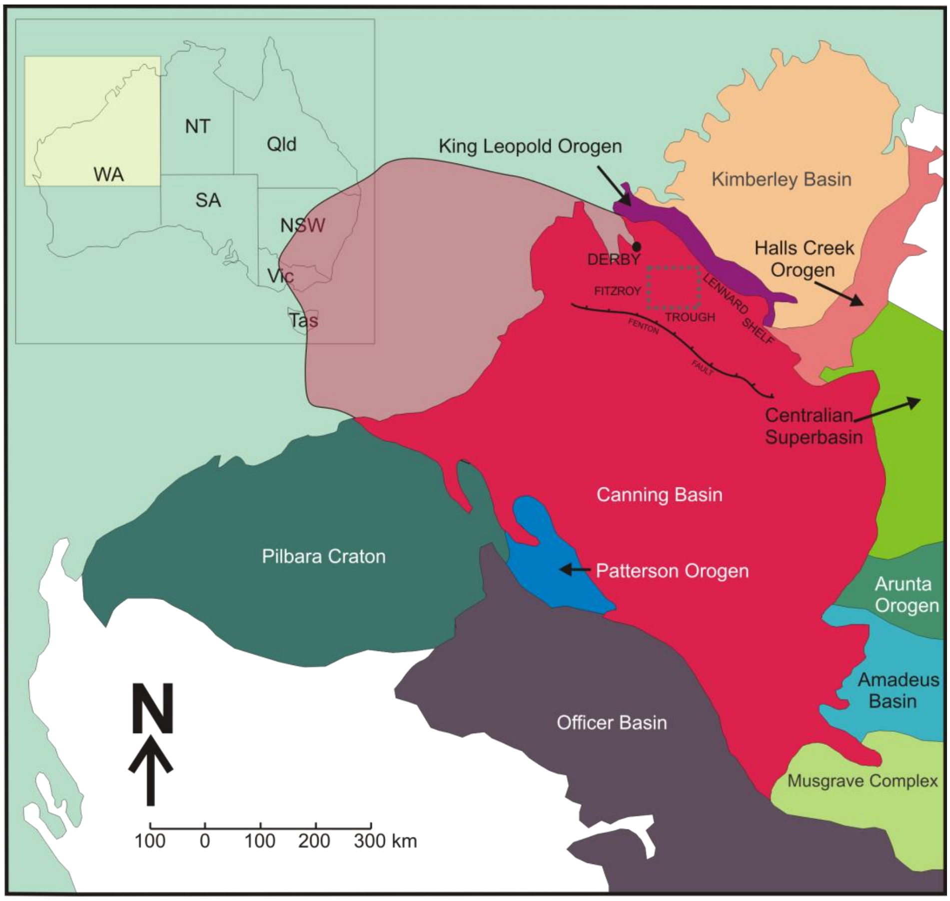

Figure 1. Map of northern Western Australia showing extent of the Canning Basin (including off-shore extent) as well as the surrounding cratons and basins. Within the Canning Basin can be seen the Fenton Fault, Fitzroy Trough and Lennard Shelf. Field work was located ~100 km south-east of Derby and can be seen as a dotted rectangle. (Adapted from McKay & Miezitis 2001)

The Erskine Sandstone Formation is of particular interest in this study as a potential host for sandstone-hosted uranium mineralisation, with sediments potentially sourced from the King Leopold Ranges. The Erskine Sandstone Formation consists mostly of very fine to fine grained sandstone and predominantly comprises of loose, coarse to fine, moderately sorted, rounded to sub-rounded quartz grains. Locally the Erskine can also contain abundant pyrite and lignite (Sloan & Neumann 1984), important in the potential uranium system as these may act as local reductants. Minor components of conglomerate and mudstone within the Erskine Sandstone Formation are interpreted to have been deposited as fluvial and deltaic sediments, representing low-temperature, near surface conditions (Reeckman 1983, Roberts 1985).

In-depth studies have not been conducted as to the exact provenance evolution of the Erskine Sandstone Formation.

This study aims to determine the provenance evolution of the Erskine Sandstone Formation and identify potential sources through U-Pb zircon analysis. This work will provide a maximum depositional age for the Erskine Sandstone Formation at its type example in the Erskine Ranges (Figure 2). Age provenance distribution diagrams will be used that identify age sources for the sediments. Finally, the similarity of provenance between the May River outcrops and the Erskine Range type section will be examined to determine whether they are conceivably from the same source.

GEOLOGICAL SETTING AND PREVIOUS WORK

Regional Geology

The Canning Basin is located in northern Western Australia and covers an area of more than 595 000 sq km (Cadman *et al.* 1993), of which 415 000 sq km is sub-aerial (Roberts 1985). Seismic surveys indicate that a thickness of up to 18 km of Ordovician to Quaternary sediments may be present in the deepest depocentre (Yeates *et al.* 1984, Cadman *et al.* 1993). The NE-SW trending intracratonic basin is bordered by the Kimberley Basin to the north, the Pilbara Craton and Officer Basin to the south, the Amadeus Basin to the east, and extending off-shore to the west (Figure 1) (Roberts 1985, Cadman *et al.* 1993).

The Canning Basin preserves a long and complex multi-phase depositional history. Commencement of deposition occurred in the early Ordovician as a result of marine transgressions from the northwest, depositing a uniform layer of sediments (Brown *et al.* 1984, Cadman *et al.* 1993, Haines & Wingate 2007). This oldest known strata of the Canning

Basin comprises clastics and carbonates that overlie a Precambrian igneous and metamorphic basement (Bretherton 1998). This strata also consists of paralic sandstones and intertidal to subtidal shales and siltstones (Cadman *et al.* 1993).

By the mid Ordovician, deposition had slowed with a period of non-deposition over the entire Canning Basin occurring from the late Ordovician to the early Silurian (Cadman *et al.* 1993). The slowed rate of deposition in the mid Ordovician resulted in fine grained clastics and carbonates, which were deposited in shallow marine to subtidal areas (Cadman *et al.* 1993).

The Canning basin may be further sub-divided into two subsidiary basins due to their distinctly different depositional histories (McWhae *et al.* 1956). These sub-basins are separated by a low basement ridge, with the part of the Canning Basin to the north of the ridge known as the Fitzroy Basin (McWhae *et al.* 1956). The name of the Fitzroy Basin, first published in 1951 (Reeves 1951), represents the same structure as the Fitzroy Trough, with the northern margins of the province matching those of the Canning Basin, and the southern margin located at the aforementioned basement ridge (McWhae *et al.* 1956). The southern part of this province also marks the southern limits of the thick Carboniferous to Triassic sequence (McWhae *et al.* 1956). For the purposes of this paper, the term Fitzroy Trough will be used, and will be focused on due to the containment of the Erskine Sandstone Formation within it.

Late Devonian rifting established the Fitzroy Trough as the major depocentre in the northern Canning Basin (Cadman *et al.* 1993). The trough was formed through movement along the Beagle Bay Pinnacle and Fenton Fault Systems, ultimately separating the trough from the Lennard Shelf (Bretherton 1998).

Uplift in the late Carboniferous resulted in a basin-wide erosional unconformity (Westphalian to Stephanian epochs) (Cadman *et al.* 1993). This uplift was relatively short-lived; basin-wide subsidence resumed in the Early Permian, facilitated by limited growth faulting in the Fitzroy Trough (Yeates *et al.* 1984, Cadman *et al.* 1993). Further tectonic activity is apparent through a low angle unconformity present between the Late Permian and Early Triassic units in the Fitzroy Trough (Cadman *et al.* 1993, Bretherton 1998), possibly a result of Late Permian rifting associated with early events in the break-up of Gondwanaland (Carey 1976).

The fine grained clastics of the Blina Shale were deposited in the Fitzroy Trough in the Early Triassic during a northwest directed marine transgression (Cadman *et al.* 1993). The Blina Shale is the basal unit of the overlying and sparsely outcropping Erskine Sandstone Formation, with the sandstone representing a subsequent marine regression in the Middle Triassic (Cadman *et al.* 1993). The Erskine Sandstone Formation consists mostly of very fine- to fine-grained sandstone and predominantly comprises of loose, course- to fine, moderately sorted, rounded to sub-rounded quartz grains. Outcrop of the Erskine Sandstone Formation is mainly restricted to the May River, and Erskine Ridge which is located 100 km south-east of Derby (Figure 2). There has been some debate as to whether the outcrop along the May River correlates with the type section located at Erskine Ridge. The shallow dipping synform shape of the Erskine Sandstone Formation is underlies a series of members and formations. The Meda Formation is most commonly associated with the Erskine Sandstone Formation (Table 1). The intermediate members and formations between the Erskine Sandstone Formation and the Meda Formation were not identified in the field area.

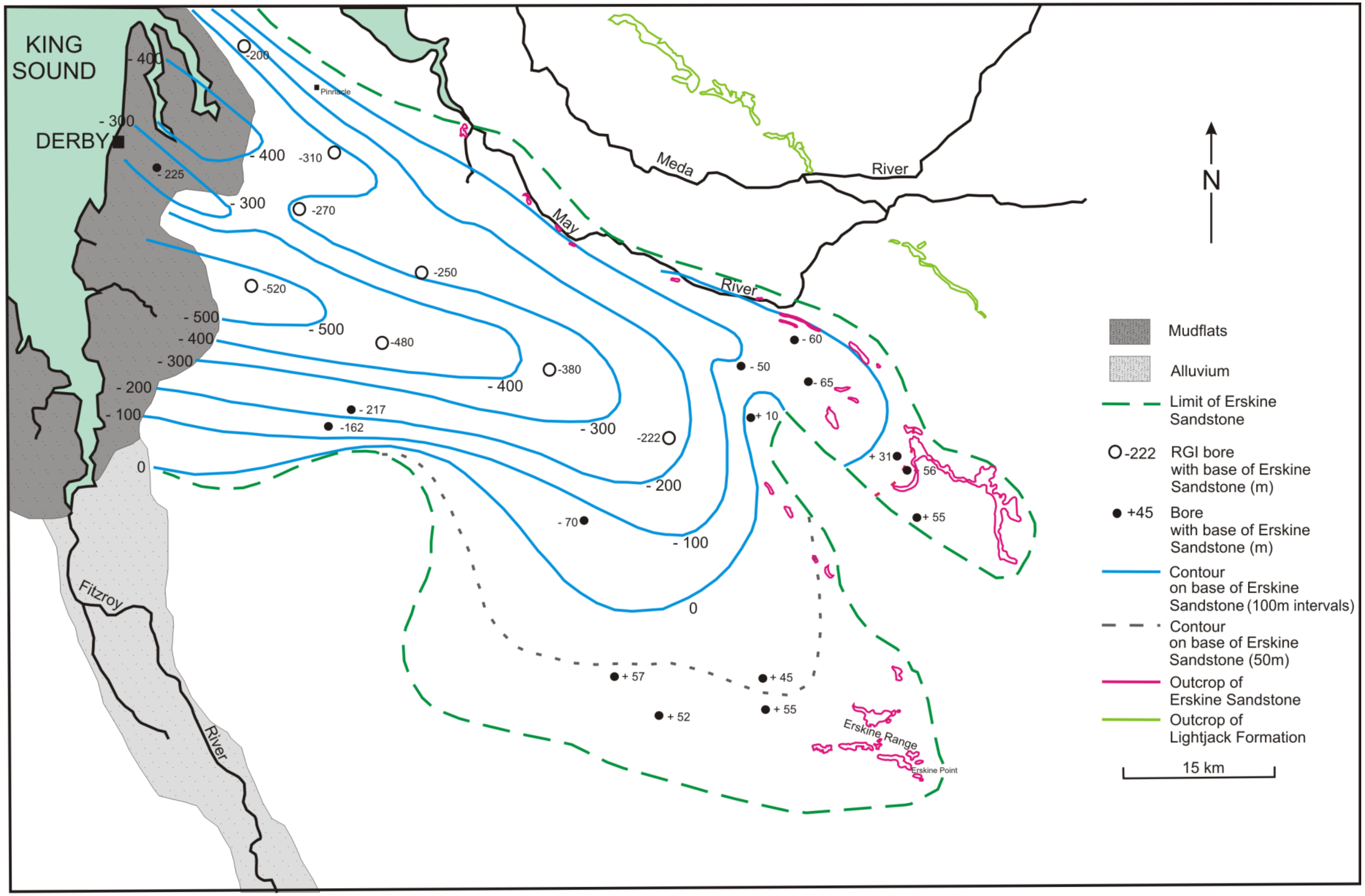

Figure 2: This figure shows the field-work area and the depth to the base of the Erskine Sandstone Formation determined through bore hole drilling. Included is outcrop of both the Erskine Sandstone Formation and the Lightjack Formation. A synformal shape can be seen trending roughly northwest-southeast. The Pinnacle Rock can also be seen north-east of Derby. Adapted from Guppy *et al.* (1980) and Lawe & Smith (1989).

Table 1: Stratigraphy of the Derby region from the Early Triassic to the Early Cretaceous, adapted from Guppy *et al.* (1980) and Smith (1989).

Period	**Formation/ Member name**	**Name abbreviation**	**Description and potential depositional environment**	**Maximum thickness**
Early Cretaceous	Melligo Sandstone	Km	Sandstone, fine to medium, well-sorted, laminated to thin-bedded; upper part silicified: **beach**	254 m (includes Meda and Jowlaenga Formations) in Jumjum 1 (Esso 1985)
Late Jurassic to Early Cretaceous	Meda Formation	Jd	Sandstone, fine to coarse; granule to pebble conglomerate; poorly sorted; cross-bedded, ripple-marked: **fluvial**	See above
	Jowlaenga Formation	Jw	Sandstone, fine to medium, well-sorted; mudstone interbeds; cross-bedded, bioturbated; minor conglomerate; fossiliferous: **shallow marine**	See above
	Jarlemai Siltstone	JKr	Mudstone, massive, bioturbated, sandy; glauconitic, phosphatic; minor limestone; fossiliferous: **deep water marine**	238 m in Fraser River Structure 1 (Goss & Crespin 1955)
Late Jurassic	Alexander Formation	Ja	Sandstone, fine to medium; interbedded mudstone; laminated to thin-bedded, lenticular bedding; ripple marked, cross-bedded; bioturbated; minor conglomerate lenses; fossiliferous: **shallow-water marine**	219 m in Fraser River Structure 1 (Goss & Crespin 1955)
Early? To Late Jurassic	Wallal Sandstone	Jl	Sandstone; minor siltstone, conglomerate, lignite.	82 m in RGI 2D (Smith 1992) 286 m in Fraser River Structure 1 (Goss & Crespin 1955)
	Mudjalla Sandstone 'Member'	Jlm	Sandstone, medium to coarse, poorly sorted, cross-bedded; siltstone, very fine sandstone, planar-bedded, ripple-marked: **fluvial**	
Early to Middle Triassic	Erskine Sandstone Formation	Re	Sandsone, very fine to fine; laminated to thin-bedded, cross-bedded, ripple marks; minor clay-pellet conglomerate; mudstone; plant fossils: **deltaic, fluvial**	265 m in RGI 9D (Lawe & Smith 1989)
Early Triassic	Blina Shale	Rb	Mudstone, sandy mudstone, laminated to thin-bedded, ripple marked, burrowed; minor fine sandstone; fossiliferous: **brackish water**	462 m in Kora 1 (Reeckman 1983)

Previous work

One of the first references to the Erskine Sandstone Formation was made by Wade (1936), when it was referred to as a member of the Erskine Series. This series also included the Blina Shale and the Meda Formation. As defined, the Erskine Series comprised of basal clays that pass into concretionary sandy shales, “soft false headed sandstones” and massive quartz conglomerates containing quartz pebbles arranged in regular bands in a coarse gritty matrix (Wade 1936). Wade (1936) also concluded that pebble bands show false bedding on a big scale and sometimes indicate the curving floors of water channels.

This initial study by Wade was followed up by Brunnschweiler (1954) who discussed the Erskine as part of his study on the Mesozoic stratigraphy of the Canning Desert. Brunnschweiler (1954) concluded that the estuarine and partly fluviatile Erskine Sandstone Formation represents the final stage of local Upper Triassic sedimentary cycle. The Erskine Sandstone Formation conformably overlies the Blina Shale, with the lower lithology of the Erskine Sandstone Formation being more of a sandy shale, similar to the upper lithology of the underlying Blina Shale (Brunnschweiler 1954).

The northern boundary of the Canning Basin has been the target of previous exploration studies for sandstone-hosted deposits. From 1978 to 1983, Afmeco Pty Ltd explored the area, selected partly because the sedimentary strata is thought to have been derived from erosion of the Halls Creek-King Leopold Orogen, which contains high levels of background uranium (McKay & Miezitis 2001). However, the exact provenance of the

Erskine Sandstone Formation and adjoining strata is not yet completely understood; there are several theories regarding the origins of the sediments.

Although the King Leopold Orogen and the Halls Creek Orogen are named separately, they form a continuously exposed V-shaped band to the south and the east of the Kimberley Basin (Figure 1) (Griffin & Grey 1990). In the Halls Creek Inlier, the age of this rapid deep crustal to supracrustal tectonic transition has been distinguished within the range 1860-1850 Ma (U-Pb zircon)(Page 1988, Tyler & Griffin 1990). The geological significance of the indicated boundary is not known. Both orogens are defined by three components: a) structurally complex areas of metamorphic and metasedimentary rocks with both intrusive and extrusive igneous rocks present that range significantly in age; b) locally restricted sedimentary successions associated with the complexes, possibly brought about by the tectonic activity of the orogens; c) folded margins with the Kimberley Basin succession also due to tectonism associated with the orogens (Griffin & Grey 1990).

Evidence from reconnaissance drilling and lithological studies of strata from this region suggests that major erosion of the Halls Creek-King Leopold Orogen took place from the Early Devonian to Early Permian (McKay & Miezitis 2001). It is thought that more than 60 per cent of the detrital material in strata of this age was derived from the erosion of the Halls Creek-King Leopold Orogen (McKay & Miezitis 2001). The depositional period of Early Devonian to Early Permian predates the Early to Middle Triassic Erskine Sandstone Formation. Although major erosion occurred prior to the formation of the Erskine Sandstone Formation, there is still potential for continued erosion to provide the detrital material for the Sandstone.

A second theory suggests that the source rocks of the Erskine Sandstone Formation were to the south. This is based on northerly current directions in the Erskine Sandstone Formation indicating a source area south of the Fenton Fault (Towner 1981). As the Fenton Fault is to the south of the Erskine Sandstone Formation this theory contradicts the first claim that the sediments were derived from the north. The Erskine Sandstone Formation is, however, widely considered to be fluvial and deltaic, allowing for multiple sediment sources (Wade 1936, Brunnschweiler 1954, McWhae *et al.* 1956, Guppy *et al.* 1980, Towner 1981, Esso 1982, Reeckman 1983, Lawe & Smith 1989, Smith 1992).

Sandstone-hosted uranium deposits and the Canning Basin

Sandstone hosted uranium deposits can be classified into tecto-lithologic, peneconcordant, and roll-front types (Dahlkamp 1978, Keats 1990). Major controls on deposition of uranium relate to the redox state, pH, ligand concentration and temperature of the aqueous fluids (Skirrow *et al.* 2009). Most of these deposits form when uranium-bearing oxidised ground water moves through sandstone aquifers and reacts with reduced materials. Therefore the location and the size of the deposits depend partly on the abundance and reactive nature of the reductant (Jaireth *et al.* 2008). Sandstones rich in organic-matter may reduce the uranium either directly with bacteria as a catalyst, or through the production of biogenic hydrogen sulphide (H_2S) (Spirakis 1996). It is also proposed that hydrogen sulphide may be produced from the interaction of oxidised groundwater with pyrite in the sandstone aquifer (Spirakis 1996, Jaireth *et* *al.* 2008). Lignite and pyrite are found in trace amounts to significant inclusions in a number of wells drilled into the Erskine Sandstone Formation (Esso 1982, Reeckman 1983, Sloan & Neumann 1984, Roberts 1985, Bretherton 1998).

There are occurrences of sandstone-hosted uranium mineralisation within the Canning Basin; the Oobagooma deposit is located in the north of the basin and is hosted by the Yampi Sandstone, an early Carboniferous sandstone (McKay & Miezitis 2001). The Yampi Sandstone was deposited in a deltaic environment influenced by tidal and fluvial processes (Botten 1984). Mineralisation is associated with organic matter and pyrite rich zones that constitute a significant component of the sandstone (McKay & Miezitis 2001). An upper band 1-5 m thick at 48-55 m deep represents a high grade zone (McKay & Miezitis 2001), where mineralisation forms a roll front deposit (Brunt 1990). The occurrence of the Oobagooma deposit suggests further sandstone-hosted uranium deposits may be present in the northern Canning Basin, as it demonstrates that conditions which promote uranium reduction and mineralisation exist.

METHODS

Sampling

A total of 24 samples were collected from two main field areas (Erskine Ridge and along the May River) at surface using a geological hammer. Through the study of the Australian 1:250 000 Geological Series maps areas which had been logged as the Erskine Sandstone Formation were able to be easily located in the field. At the Erskine Ridge, the aim was to collect samples from areas which have previously been logged as the Erskine Sandstone Formation, Blina Shale and the Meda Formation. In the May

River field area, the goal was to collect sandstone samples previously logged as the Erskine Sandstone Formation. Before the samples were taken, their GPS locations were recorded and the rock was logged in-situ. The GPS coordinates and geological logs can be found in Appendix A.

Gamma-ray spectrometer and scintillometer

An RS-230 BGO Super-Spec Spectrometer (SPP) with a 300 second count time was used on petroleum well cutting sample composites. The spectrometer measured for potassium (K), uranium (U) and thorium (Th) and a total count value. A scintillometer (SPP and measuring peak count) was used in the field across the Erskine Sandstone Formation and Blina Shale boundary, count time varied until the reading was stabilised.

U-Pb zircon LA-ICP-MS geochronology

Zircon geochronology was used to help constrain the maximum depositional age of sediments, and to further assist a provenance study. To allow for U-Pb zircon analysis using Laser Ablation Inductively Coupled Plasma Mass Spectrometry (LA-ICP-MS), samples were crushed and milled using a ring-mill. Zircons were separated from a 79 µm to 425 µm sieved fraction using standard panning, Frantz isodynamic magnetic and methylene-iodide separation techniques, followed by handpicking (Payne *et al.* 2010). Zircons were mounted on circular epoxy mounts and hand polished to reveal the centre of the zircons.

Scanning Electron Microscope (SEM) imaging was completed using a Phillips XL20 SEM instrument at Adelaide Microscopy, University of Adelaide. This instrument is equipped with an energy dispersive X-Ray spectrometer (EDAX) and back-scattered electron (BSE) detector. The BSE function allowed a zircon map to be constructed through stitching together several board images of the mount. After the generation of a map, cathodoluminescence permitted for zircon grains to be imaged and characterised for fractures and zonations (Griffin *et al.* 2004). Zonations may be present and suggest multiple age components, with homogeneous areas greater than 30 µm needed for an LA-ICPMS spot size.

Uranium-lead isotopic analyses were conducted at Adelaide Microscopy, using a New Wave 213 nm neodymium-YAG laser coupled to an Agilent 7500cs ICP-MS in a helium (He) ablation atmosphere. Each analysis comprised an acquisition time of 120 s. Included within this time is 30 s of background measurement, 10 s of laser firing with the shutter closed allowing for crystal and beam stabilisation, and 80 s of laser ablation of the zircon. A beam with a surface diameter of 30 µm, repetition rate of 5 Hz and laser intensity of 9-10 J/cm^2 was used for this purpose (Payne *et al.* 2006). Multiple dwell times were used for the differing isotope masses (10 ms, 15 ms, 30 ms, 10 ms, 10 ms, 15 ms for ^{204}Pb, ^{206}Pb, ^{207}Pb, ^{208}Pb, ^{232}Th, ^{235}U and ^{238}U respectively).

Correction to the U-Pb fractionation was corrected using an external zircon standard, GJ (TIMS normalisation data: ^{207}Pb/^{206}Pb age = 607.7 ± 4.3 Ma; ^{206}Pb/^{238}U age = 600.7 ± 1.1 Ma; ^{207}Pb/^{235}U age = 602.0 ± 1.0 Ma (Jackson *et al.* 2004)). The accuracy of data correction was assessed though the repeated analysis of an internal zircon standard, Plešovice (ID-TIMS normalisation data ^{207}Pb/^{206}Pb age = 337.13 ± 0.37 Ma (Slama *et al.* 2008)). Data reduction was performed using 'GLITTER' software developed at Macquarie University, Sydney (Griffin *et al.* 2008). Throughout the analysis of samples, the weighted averages obtained for GJ are $^{207}Pb/^{206}Pb$ age = 609.0 ± 3.3 Ma (n = 485, MSWD = 0.49); $^{206}Pb/^{238}U$ age = 600.89 ± 0.66 Ma (n = 485, MSWD = 4.7); $^{207}Pb/^{235}U$ age = 602.45 ± 0.73 Ma (n = 485, MSWD = 2.6) and Plešovice are $^{207}Pb/^{206}Pb$ age = 373.7 ± 5.9 Ma (n = 296, MSWD = 6.1); $^{206}Pb/^{238}U$ age = 333.91 ± 0.66 Ma (n = 296, MSWD = 17); $^{207}Pb/^{235}U$ age = 338.62 ± 0.80 Ma (n = 296, MSWD = 11.5). The reduced data was then exported into Microsoft Excel from which conventional concordia, weighted average plots and probability density plots were generated using Isoplot v4.11 (Ludwig 2003). All errors stated in data tables and alongside concordia diagrams are at a 1σ level. Concordancy was calculated by using the ratio of $^{206}Pb/^{238}U$ with $^{207}Pb/^{206}Pb$. All geochronological data from this study can be found in Appendix B.

OBSERVATIONS AND RESULTS

Field observations of the Erskine Sandstone Formation

Complete field observations of the Erskine Sandstone Formation outcrop can be found in Appendix C. Two stratigraphic columns were taken in the field at the Erskine Ridge (Figure 3 – 4).

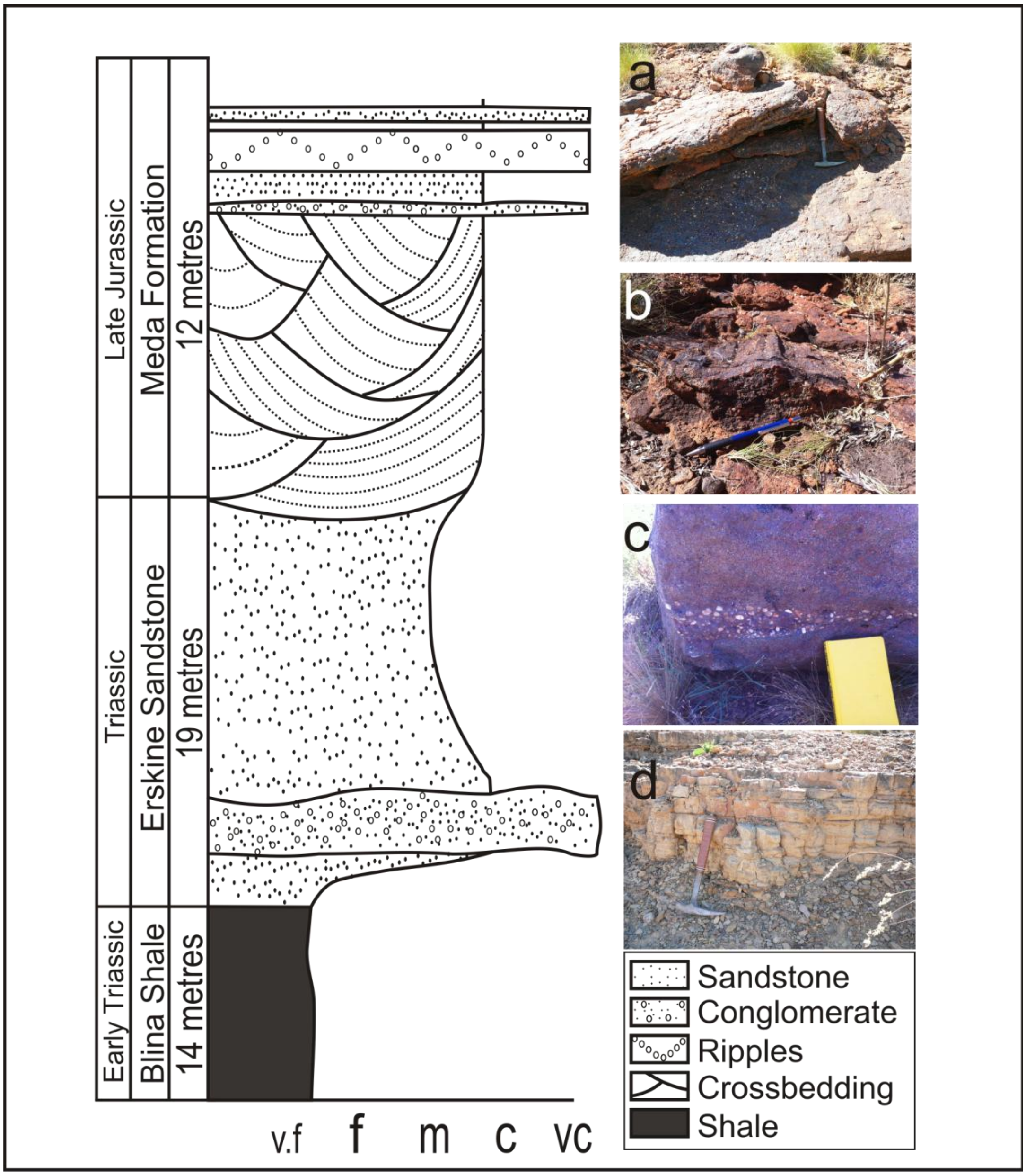

Figure 3. Stratagraphic column taken at Erskine Ridge north of the Great Northern Highway at location 642278 mE, 8026369 mN (x-axis = grain size, v.f = very fine, f = fine, m = medium, c = coarse, vc = very coarse); (a) Conglomerate layer; (b) Preserved ripples; (c) Coarse-grained infill;, and (d) Blina Shale.

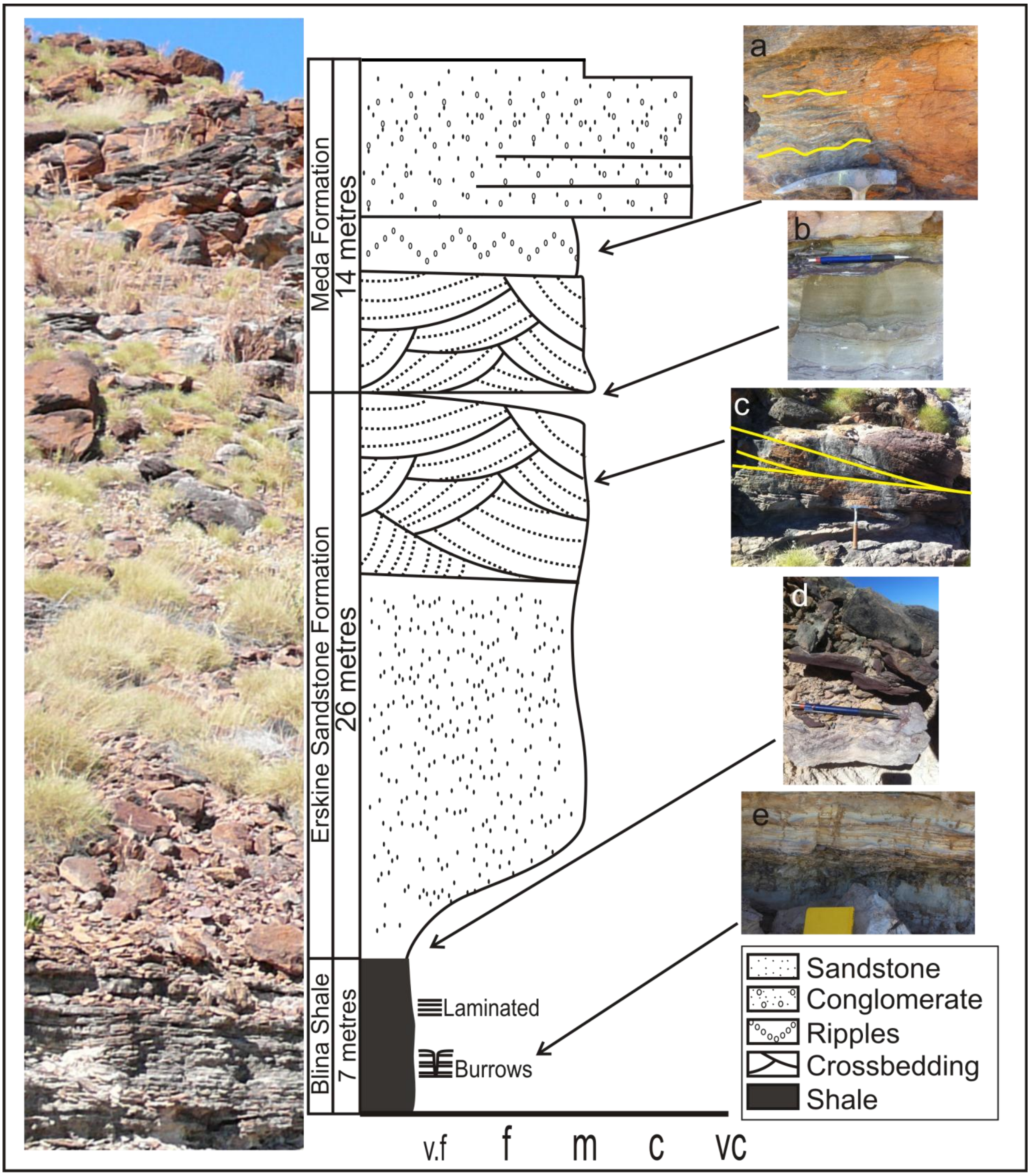

Figure 4. Stratigraphic column taken at the type section at Erskine Point within the Erskine Range, south of the Great Northern Highway at location 643514 mE, 8025584 mN. The picture to the left of the column represents an approximate scale image of the outcrop. (x-axis = grain size, v.f = very fine, f = fine, m = medium, c = coarse, vc = very coarse); (a) Ripples present; (b) Fine-grained unconformity layer; (c) Cross-bedding; (d) Unconformity layer between the Blina Shale and the Erskine Sandstone Formation;, and (e) Burrows present in the Blina Shale.

Geological logs of petroleum wells

Drillhole cuttings were examined in the Geological Survey of Western Australia's Perth core library. The cuttings were sourced from three petroleum wells (East Yeeda 1, West Kora 1 and Booran 1) which intersected the Erskine Sandstone Formation and the Blina Shale. Samples were presented in ~100–200 g, 5–10 m composites. Full geological logs can be found in Appendix D. A gamma-ray spectrometer was used on these cuttings (Figure 5) to attempt to determine formation boundaries, while a scintillometer was used in the field for this purpose (Figure 6).

EAST YEEDA 1

The East Yeeda 1 hole was sampled in 5 m composites samples, giving a relatively inaccurate representation of the stratigraphy and not allowing for any structural measurements. Due to a distinct change in colour from red/orange to a red/black colour, a boundary could be inferred to be at a depth of 55-60 m. This is matched by the lithological notes in the well completion log (Roberts 1985), which mention a boundary occurring at 54 m between the Erskine Sandstone Formation and the Blina Shale. The change only occurs in colour, with grain size not altering, contrary to what would be expected in a change from shale to sandstone. The cuttings from the Erskine Sandstone Formation were moderately sorted and predominantly sub-angular and of varying mineral composition.

The East Yeeda 1 geological log mentions a concrete contamination occurring from 145-200 m, which masks the lithology (Roberts 1985). While there is no mention as to the degree of contamination, upon studying this interval the contamination makes it difficult to determine the percentages of the components. Further to this, the fine-grained shale seen in the field is not generally represented in the samples until 200 m depth, after the contaminated zone.

WEST KORA 1

West Kora 1 is similar to the East Yeeda 1 hole in that there appears to be an upper coarser layer to the Blina Shale, and a siltier lower layer. The siltier lower layer appears to occur at ~170m depth and has a uniform composition. The upper layer has a mixed composition and a varying grain size.

Overall the Erskine Sandstone Formation is red in colour, has a varying grain size but predominantly medium grained with some coarse grains, well sorted, sub-round to sub-angular.

BOORAN 1

The section of the Booran 1 hole targeted was an interpreted boundary between the Erskine Sandstone Formation and the Blina Shale. The section was predominantly poorly sorted, with the quartz composition dropping at depth. The transition occurred into soft clasts of fine-grained sediments.

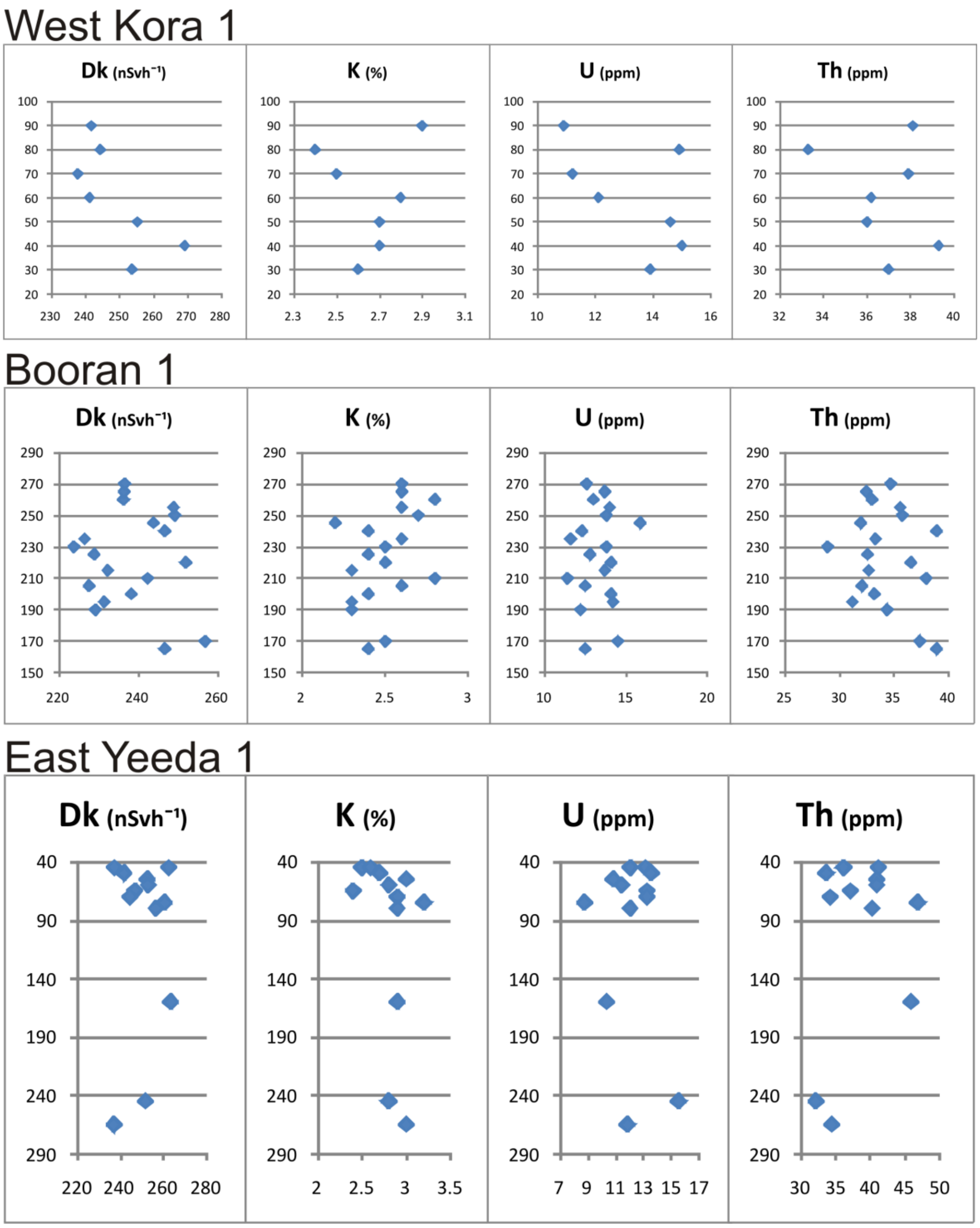

Figure 5. Gamma-ray spectrometer measurements taken of the petroleum well-hole cutting samples. No distinct patterns were evident between the Erskine Sandstone Formation and the Blina Shale. The x-axis represents the respective element readings while the y-axis gives hole depths. All measurements can be found in Appendix E

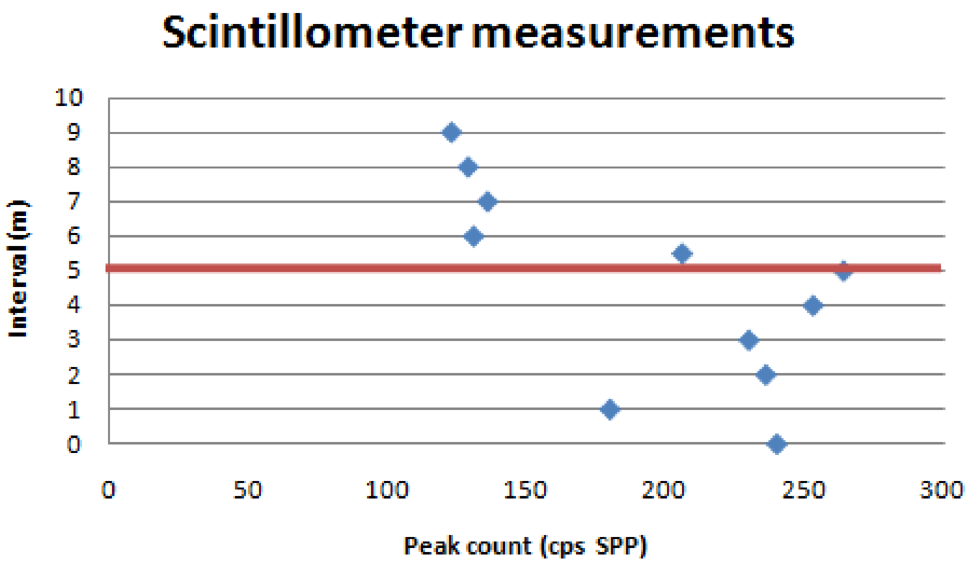

Figure 6. Scintillometer measurements taken at Erskine Point within the Erskine Range over a contact zone between the Erskine Sandstone Formation and the Blina Shale, showing lower readings within the Erskine Sandstone Formation. The red line represents the contact area. The 0 m interval is at 106 m above sea level. All measurements can be found in Appendix F.

Geochronology

Uranium-lead analyses were conducted on nine samples and are listed in Table 2.

Table 2. All samples used for geochronological purposes.

Sample name	Northing (mN)	Easting (mE)	Comments
1-02	8028194	635367	ESF conglomerate NW of the Erskine Range
3-06	8025570	643507	ESF Erskine Point
3-08	8025565	643510	Cross-bedded layer within the ESF at Erskine Point
3-09	8053634	648703	Highly ferruginised outcrop – ESF at Erskine Point
4-11	8088734	601396	Outcrop at May River – Fe rich
4-12	8088734	601396	Outcrop at May River – less oxidised
4-13	8093267	585105	Pinnacle Rock outcrop – fine grained
4-14	8093267	585105	Pinnacle Rock outcrop – conglomerate
5-18	8025561	643505	Oxidised and bleached rock at Erskine Point

Included in the table are the location coordinates as well as comments on the rock. (ESF = Erskine Sandstone Formation, Fe = Iron)

Probability density plots from the Erskine Range can be seen in Figure 7, while Figure 8 shows probability density plots from the May River outcrops. Figure 9 presents a combined provenance figure. Figures 10 – 12 present concordia plots with example zircons from each respective sample.

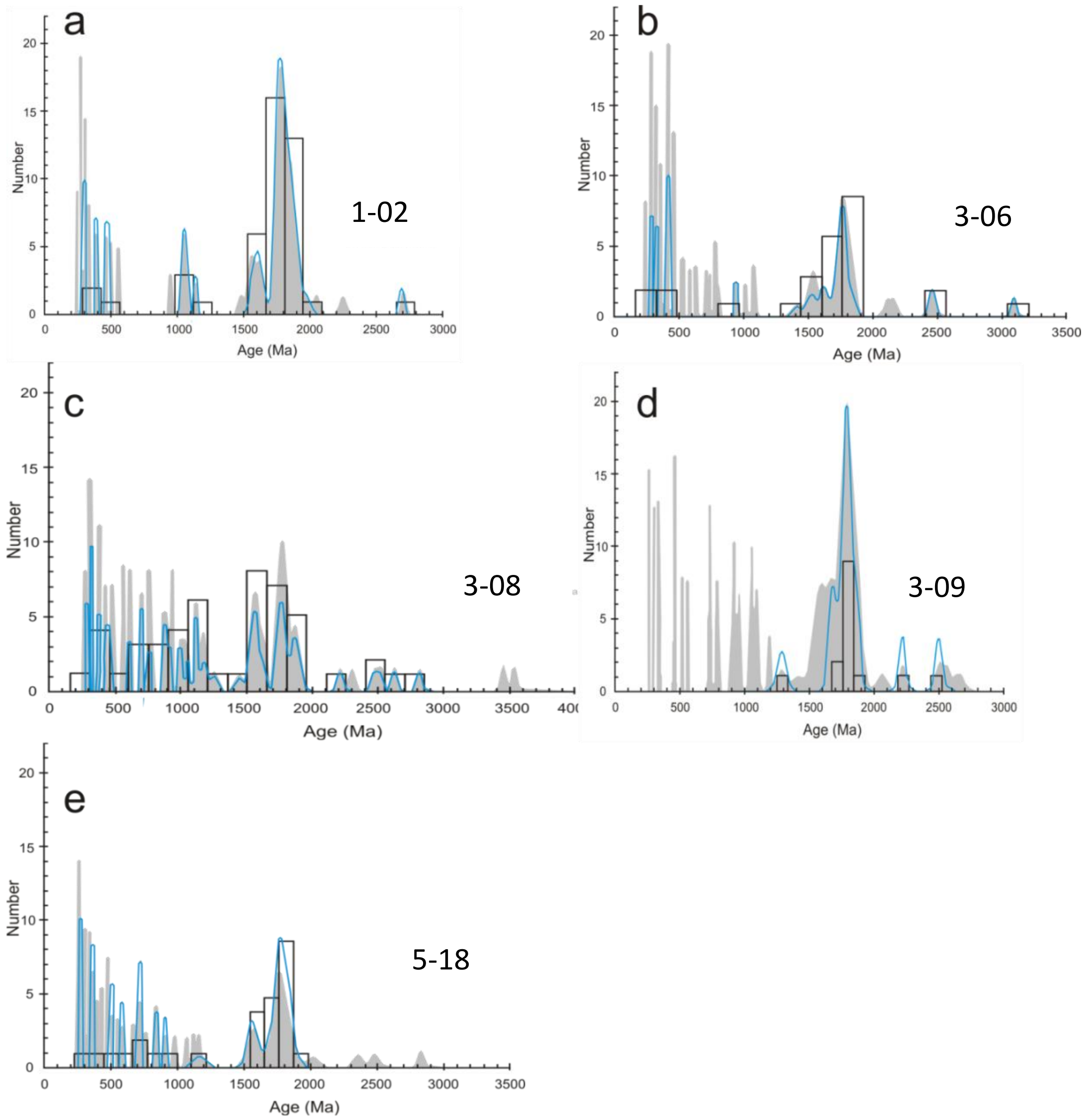

Figure 7. Probability density plots of the samples taken from the Erskine Range. The grey represents all the data with the blue outline representing 90-110% concordant data. The histogram represents the number of concordant samples within the respective age brackets.

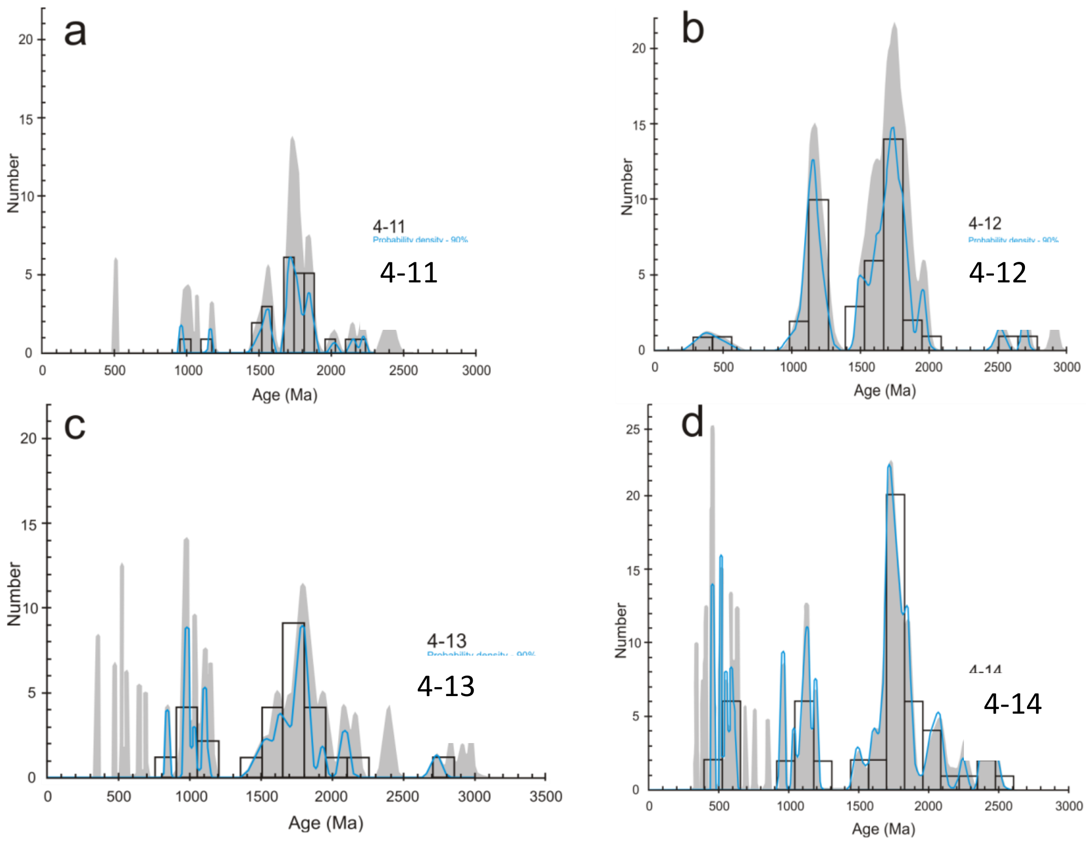

Figure 8. Probability density plots of the samples taken from the May River outcrop. The grey represents all the data with the blue outline representing 90-110% concordant data. The histogram represents the number of concordant samples within the respective age brackets.

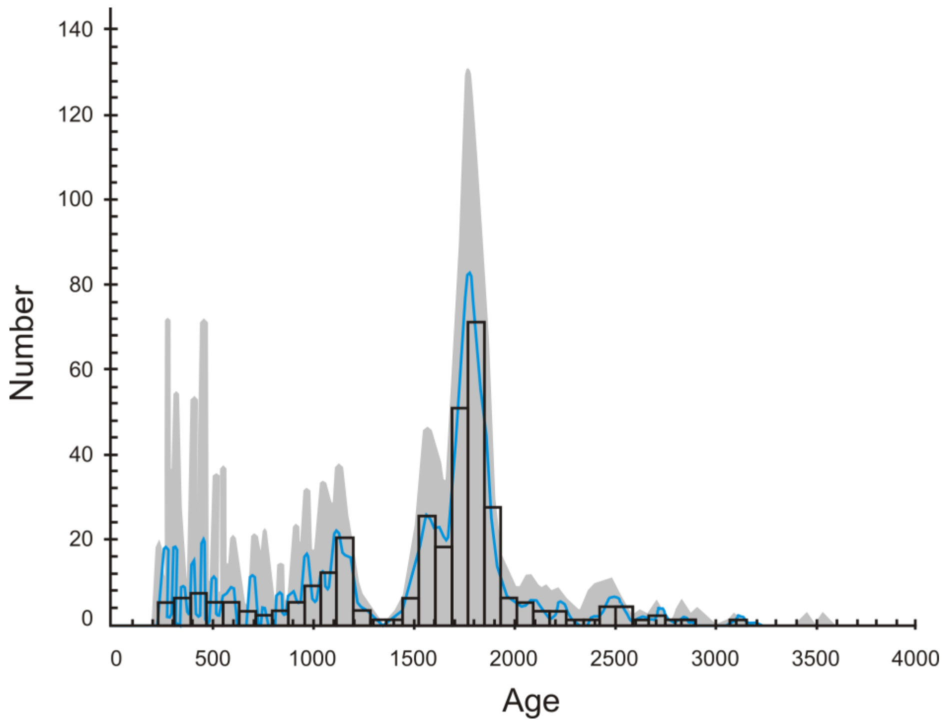

Figure 9. Probability density plot of all sample data (grey) with the blue line representing all data with a concordancy between 90-110%.

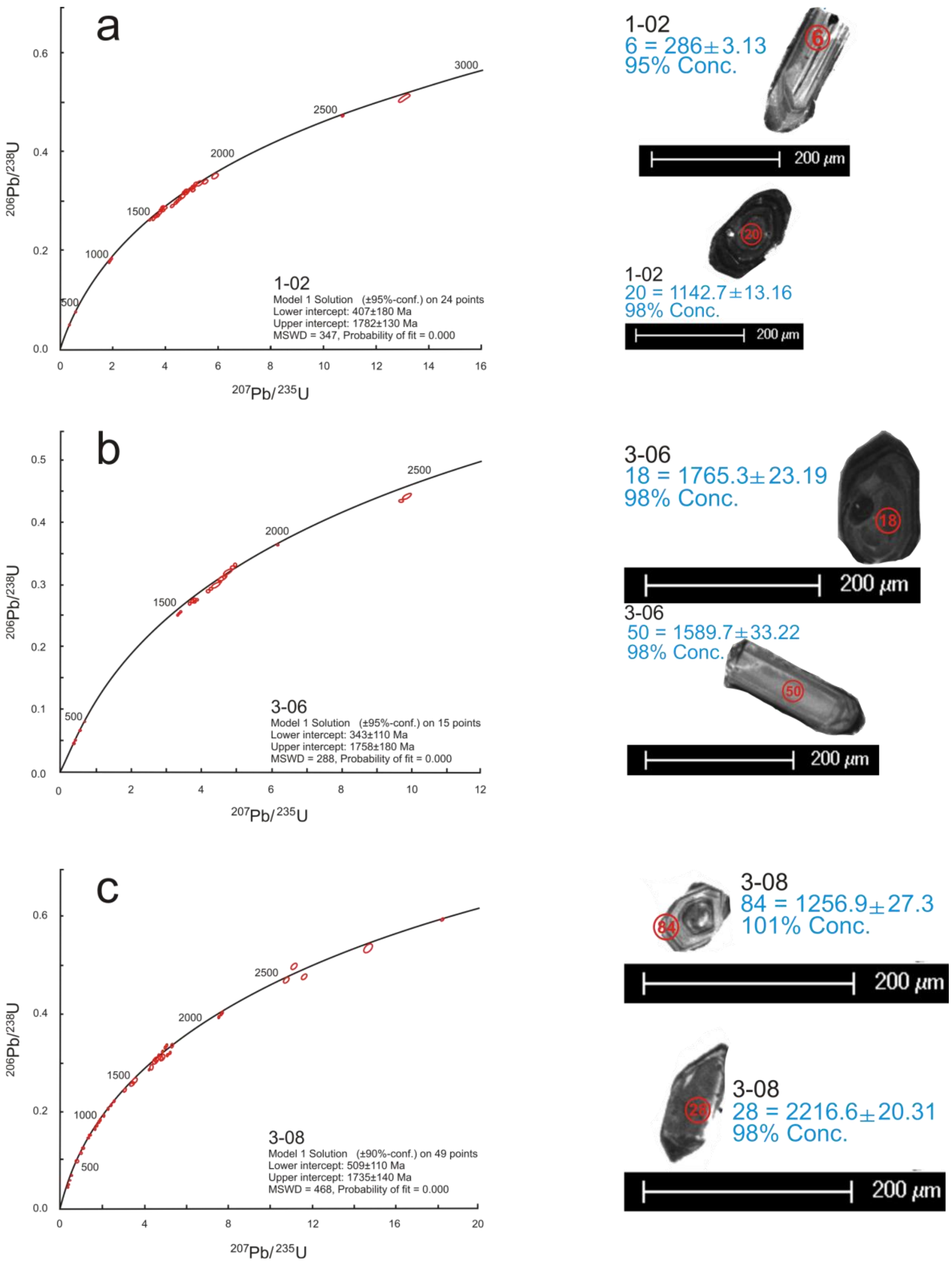

Figure 10. U-Pb concordia plots with CL images of zircons from the sample, the number within the circle represents the LA-ICPMS spot number.

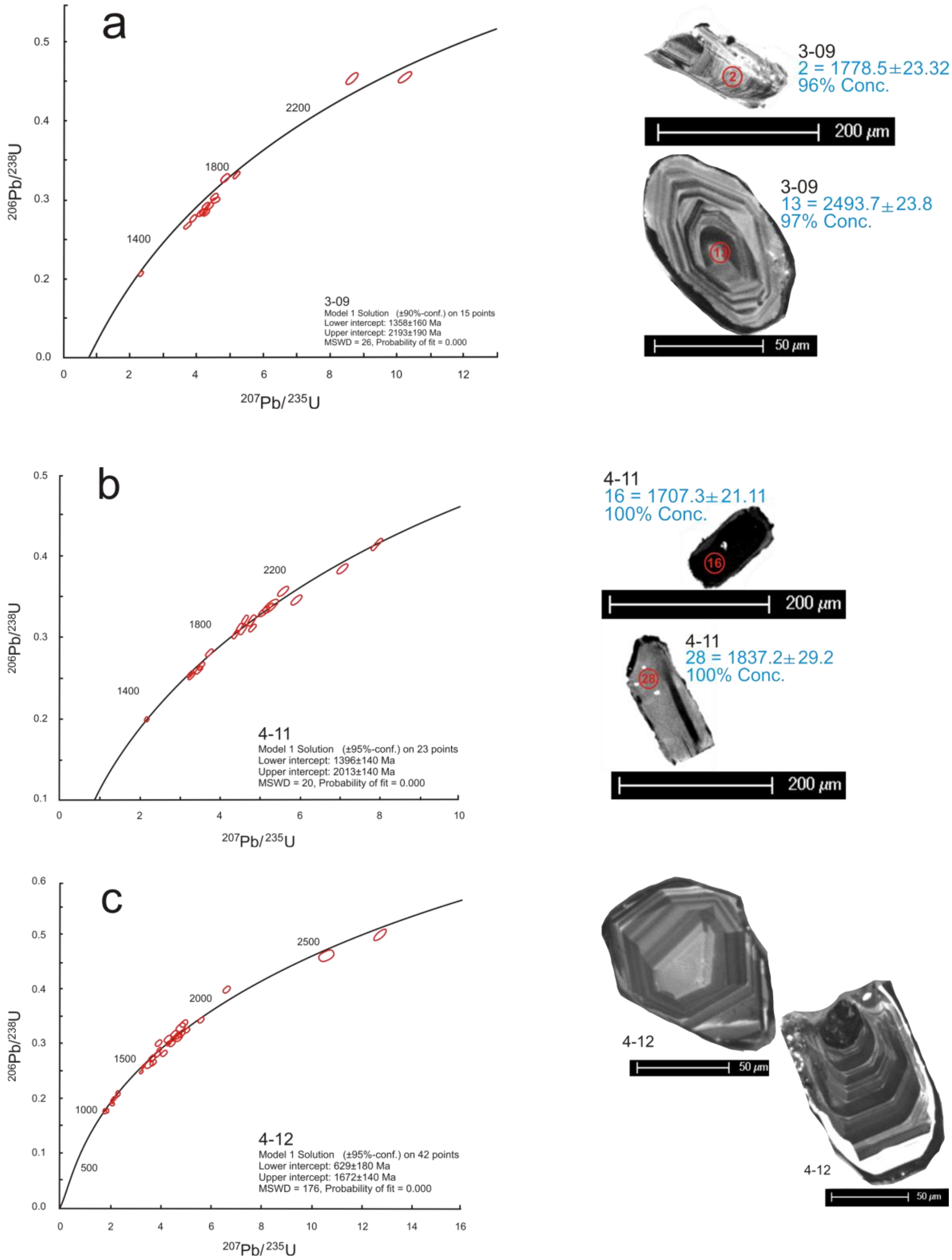

Figure 11. U-Pb concordia plots with CL images of zircons from the sample, the number within the circle represents the LA-ICPMS spot number.

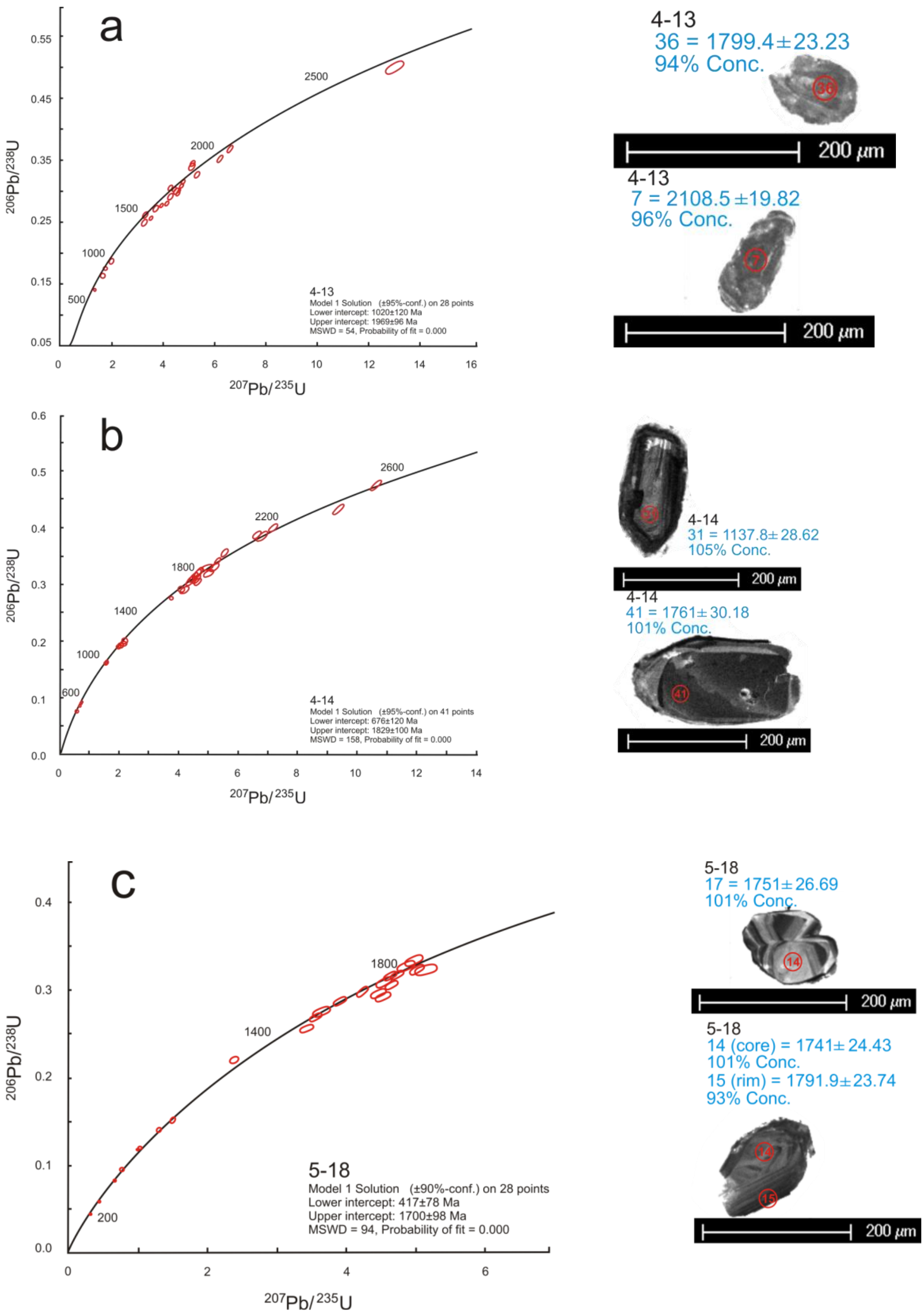

Figure 12. U-Pb concordia plots with CL images of zircons from the sample, the number within the circle represents the LA-ICPMS spot number.

Sample 1-02

Sixty-five analyses were conducted on 63 individual zoned zircon grains mounted in epoxy resin (Figure 10a). Twenty were rejected due to falling outside of 90-110% concordance and one was not used for having high common lead. The U-Pb concordia plots were used to plot these analyses (Figure 10a). The probability density plots (Figure 7a) showed concordant zircon age concentrations and provenance peaks at 300-600 Ma, 1000-1100 Ma, 1500-2100 Ma and 2700-2800 Ma. The youngest 90-110% concordant zircon age was 307.1 ± 3.7 Ma.

Sample 3-06

Seventy-eight analyses were conducted on 77 individual zoned zircon grains mounted in epoxy resin (Figure 10b). Forty-nine were rejected due to falling outside of 90-110% concordance and nine were not used for having high common lead. The U-Pb concordia plots were used to plot these analyses (Figure 10b). The probability density plots (Figure 7b) showed concordant zircon age concentrations and provenance peaks at 350-450 Ma, 900 Ma, 1300-1900 Ma, 2450 Ma and 3100 Ma. The youngest 90-110% concordant zircon age was 289.5 ± 3.42 Ma.

Sample 3-08

Eighty-three analyses were conducted on 82 individual zoned zircon grains mounted in epoxy resin (Figure 10c). Twenty-nine were rejected due to falling outside of 90-110% concordance and seven were not used for having high common lead. The U-Pb concordia plots were used to plot these analyses (Figure 10c). The probability density plots (Figure 7c) showed concordant zircon age concentrations and provenance peaks from 300-2000 Ma, 2200 Ma, 2400-2700 Ma and 2800 Ma. The youngest concordant zircon age was 322.6 ± 4.75 Ma.

Sample 3-09

Seventy analyses were conducted on 70 individual zoned zircon grains mounted in epoxy resin (Figure 11a). Fifty-three were rejected due to falling outside of 90-110% concordance and two were not used for having high common lead. The U-Pb concordia plots were used to plot these analyses (Figure 11a). The probability density plots (Figure 7d) showed concordant zircon age concentrations and provenance peaks at 1300 Ma, 1600-2000 Ma, 2200 Ma and 2500 Ma. The youngest concordant zircon age was 1286.6 ± 21.47 Ma.

Sample 4-11

Forty-eight analyses were conducted on 48 individual zoned zircon grains mounted in epoxy resin (Figure 11b). Eight were rejected due to falling outside of 90-110% concordance and eight were not used for having high common lead. The U-Pb concordia plots were used to plot these analyses (Figure 11b). The probability density plots (Figure 8a) showed concordant zircon age concentrations and provenance peaks at 1200 Ma and 1500-2300 Ma. The youngest concordant zircon age was 1173.6 ± 12.85 Ma.

Sample 4-12

Sixty-two analyses were conducted on 62 individual zoned zircon grains mounted in epoxy resin (Figure 11c). Seventeen were rejected due to falling outside of 90-110%

concordance and two were not used for having high common lead. The U-Pb concordia plots were used to plot these analyses (Figure 11c). The probability density plots (Figure 8b) showed concordant zircon age concentrations and provenance peaks at 500 Ma, 900-2100 Ma and 2400-2800 Ma. The youngest concordant zircon age was 486.1 ± 77.7 Ma.

Sample 4-13

Seventy analyses were conducted on 70 individual zoned zircon grains mounted in epoxy resin (Figure 12a). Thirty-five were rejected due to falling outside of 90-110% concordance and eight were not used for having high common lead. The U-Pb concordia plots were used to plot these analyses (Figure 12a). The probability density plots (Figure 8c) showed concordant zircon age concentrations and provenance peaks at 800-1200 Ma, 1400-2200 Ma and 2700 Ma. The youngest concordant zircon age was 843.3 ± 9.8 Ma.

Sample 4-14

Eighty-one analyses were conducted on 79 individual zoned zircon grains mounted in epoxy resin (Figure 12b). Nineteen were rejected due to falling outside of 90-110% concordance and four were not used for having high common lead. The U-Pb concordia plots were used to plot these analyses (Figure 12b). The probability density plots (Figure 8d) showed concordant zircon age concentrations and provenance peaks at 400-650 Ma, 900-1250 Ma, 1600-2200 Ma and 2400-2600 Ma. The youngest concordant zircon age was 467.4 ± 8.08 Ma.

Sample 5-18

Sixty-four analyses were conducted on 62 individual zoned zircon grains mounted in epoxy resin (Figure 12c). Thirty-one were rejected due to falling outside of 90-110% concordance and six were not used for having high common lead. The U-Pb concordia plots were used to plot these analyses (Figure 12c). The probability density plots (Figure 7e) showed concordant zircon age concentrations and provenance peaks at 250-1000 Ma, 1200 Ma and 1500-2000 Ma. The youngest concordant zircon age was 275.2 ± 3.43 Ma.

DISCUSSION

Field observations of the Erskine Sandstone Formation

The Erskine Sandstone Formation varied from outcrop in terms of: grain size, sorting, features and levels of ferrugination. Grain size varied from <1 mm in some areas to up to 5 mm and were generally sub-angular to sub-rounded, with larger grains generally accompanied by conglomeritic layers comprised of sub-angular quartz ranging in size. The angular nature of the clasts suggests a rapid deposition rate due to their minimal rounding. Further to this, it suggests that they were not transported a long distance and were therefore deposited close to their origin. Sections of bleached and oxidised layered sandstone are present only within the Erskine Sandstone Formation at Erskine Point. This unique feature may however be a more common feature that has been masked in other areas by significant ferrugination of outcrop, which is common in most low-lying outcrop and sub-outcrop. The accumulation of coarser material within a majority of finer sediments suggests a fluvial to deltaic depositional system, supporting previous work in the area.

The field study of the area around the township of Derby focusing of the Erskine Sandstone Formation, Blina Shale and the Meda Formation has resulted in several key aspects for further work, most notably a further method of identifying the Erskine Sandstone Formation in the field. Due to the Erskine Sandstone Formation having an upper coarser section and a lower siltier section, similar to that of the Blina Shale, identification of the lower aspect of the Erskine is made difficult by the similarities between the siltier section of the Erskine, and the mudstone of the Blina Shale (Figures 3 – 4). Further to the problem of identifying the Erskine, the upper limits of the Erskine is hard to define as it is mostly overlain by the Meda Formation, a sandstone with similar characteristics.

Identification of the Erskine Sandstone Formation can however be made through the use of wire-line logs, and is seen as one of the most definite way to determine the base of the Erskine Sandstone Formation. While the use of a gamma-ray spectrometer on the cuttings from the holes West Kora 1, Kora 1 and West Booran 1, did not help in identifying the boundary between the Erskine Sandstone Formation and the Blina Shale (Figure 5), the use of a scintillometer in the field, did. The counts per second (SPP) were higher while measuring the Blina Shale, the highest at a potential contact boundary between the Blina Shale and the Erskine Sandstone Formation, and dropped significantly once into the Erskine Sandstone Formation (Figure 6). Limited scintillometer measurement prevented delineation of potential contact zones.

Petroleum well cuttings

The fine-grained Blina Shale seen in the field is generally not represented in the petroleum well cutting samples until 200 m depth in the Kora 1 hole. This could suggest that the assumed Erskine-Blina boundary at 54 m could be a change from the Erskine Sandstone Formation into a different group which is present between the Erskine Sandstone Formation and the Blina Shale. On the other hand, if it is all Blina Shale then it could be separated into two distinct groups; (I) An upper coarser silt-sand which is darker in colour, generally dark red/black; (II) A lower silt-dominated section which is grey in colour. This therefore suggests that the Blina Shale gradually coarsens upwards into the Erskine Sandstone Formation with a change that corresponds with the end of the concrete contaminated zone at 200 m. This coarser sandier section could be a source of confusion in labelling and identifying subgroups around the Blina Shale and Erskine Sandstone Formation. The grain size, sub-angular to sub-rounded shape and iron staining seen in the Erskine Sandstone Formation in the field were represented in the cuttings of these three analysed petroleum wells.

Geochronology

The maximum depositional age can be determined as being younger than the youngest 90-110% concordant zircon age. Two distinct maximum depositional age groups are present, which correlate with one group being from the Erskine Ranges, and one group being from the May River outcrop. The maximum deposition age for the Erskine Range samples were 290 Ma, 289 Ma, 322 Ma, 275 Ma and 1286 Ma, however several ages were present in this sample from 263-350 Ma but with a lower concordant value (for samples 1-02, 3-06, 3-08, 5-18 and 3-09 respectively). The maximum depositional age for the May River outcrop samples were 486 Ma, 467 Ma, 843 Ma with several ages at

500 Ma with a lower concordant value, and 1173 Ma with similar ages with lower concordancy (for samples 4-12, 4-14, 4-13 and 4-11 respectively). These two distinct maximum depositional age groups from the two distinct outcrop locations suggest that the samples from the Erskine Ranges had younger sources.

Tectonic activity present in the Late Permian and Early Triassic (Cadman *et al.* 1993, Bretherton 1998), evident by a low angle unconformity, may provide a model for the differing maximum depositional ages between the May River outcrop and the Erskine Range outcrop. This tectonic activity, or another deformation/rift event, possibly as a result of Late Permian rifting associated with the early events of the break-up of Gondwanaland (Carey 1976), could expose Permian aged rocks. The differing maximum depositional ages suggests different sources. Rifting, or a deformation event, may have resulted in one source containing Permian aged sediments which are contained within the Erskine Ridge. Another source containing Mesoproterozoic rocks may have eroded to be contained within the May River outcrops.

Throughout this study, many near concordant zircon analyses were obtained and can be interpreted to have experienced Pb loss in response to various geological processes (Whitehouse & Kemp 2010). This is evident in Figures 7 and 8, where non-concordant data is present as a range of ages. While this series of data is often backed up through the presence of concordant ages, distinct trends can be seen throughout all the samples (Figure 13).

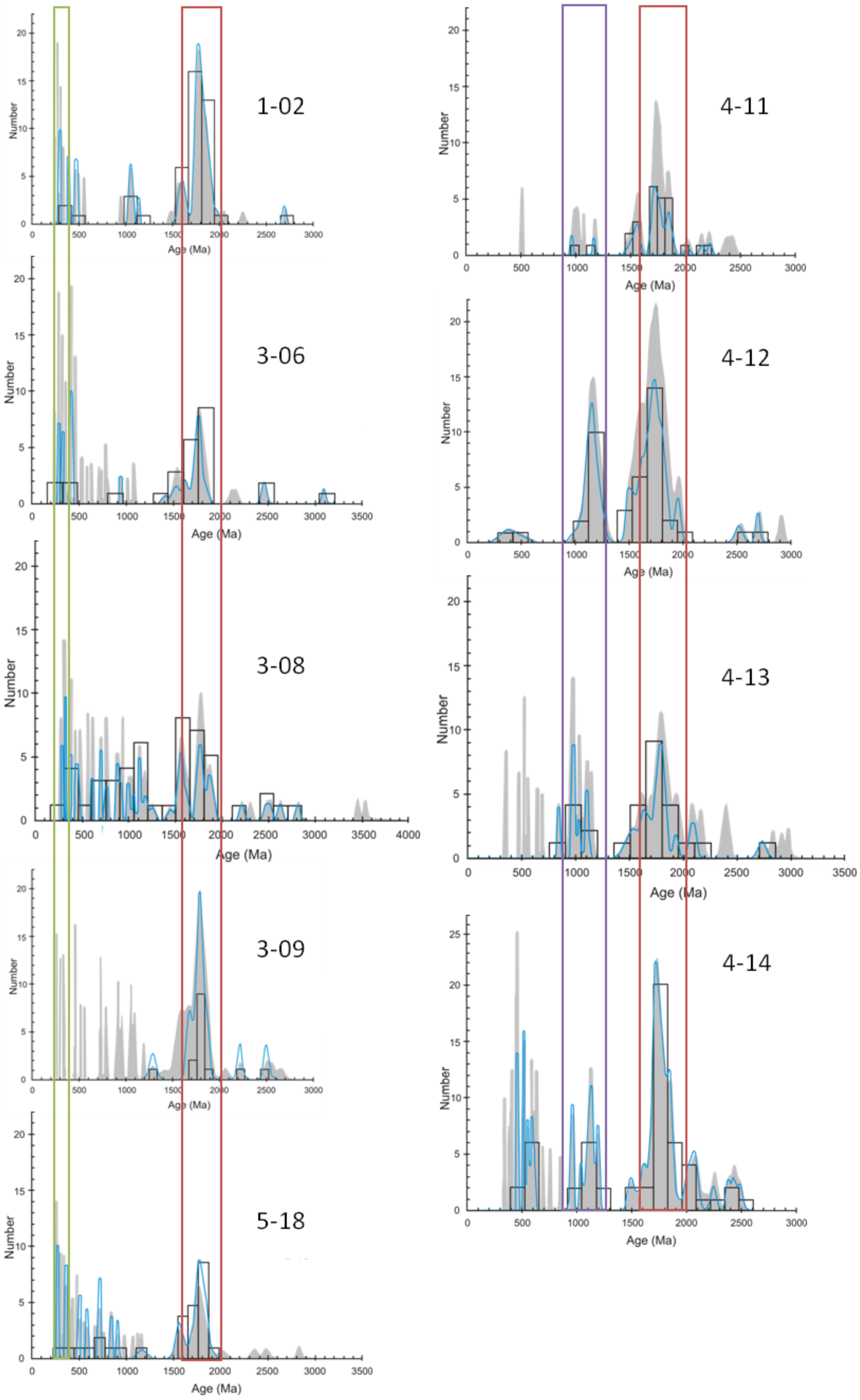

Figure 13. All probability density plots displayed with aligned ages. The left column represents the Erskine Range samples, the green box highlights the Permian aged zircons present. The right column represents the May River outcrops with the Mesoproterozoic zircons highlighted in purple. Both have the Palaeoproterozoic zircons highlighted in red.

Several samples (1-02, 3-06, 3-08, 3-09, 4-12, 4-13 and 4-14) contained within them 90-110% concordant Archaean aged zircons. A possible source of Archaean aged rocks is the Marymia Inlier, central Western Australia, as it is thought that the Inlier supplied detritus to the adjacent basins (Vielreicher & McNaughton 2002). Recent studies indicate the area was intruded by high-level, felsic to intermediate porphyries at 2694 ± 7 Ma and potentially also at 2660 ± 4 Ma (Vielreicher & McNaughton 2002). Most authors propose the Inlier to be Archean and to be part of the Yilgarn Craton that was uplifted, rotated and reworked in the Proterozoic (Muhling *et al.* 1976, Gee 1987, Pirajno *et al.* 1995, Occhipinti *et al.* 1998, Pirajno & Occhipinti 2000, Vielreicher & McNaughton 2002).

A large population peak is evident in the early to middle Palaeoproterozoic (Figure 9), indicating that a significant amount of the sediment in the area was provided by the erosion of 1500-2000 Ma rocks.

A potential source of Palaeoproterozoic rocks could be the King Leopold Ranges, located to the north and east of the Fitzroy Trough and consequently, the Erskine Sandstone Formation. These ranges are predominantly comprised of 1500-2000 Ma rocks. Included within this age bracket are the Speewah Group, Kimberley Group, Whitewater Volcanics and the Lamboo Complex which consist of granites and volcanics (Catography Services Branch 1993).

The Musgrave block (Figure 1) may be a potential source of Mesoproterozoic sediments as a result of several events. These events include extensive felsic magmatism, which occurred in the Musgrave Block between 1200 and 1150 Ma (White *et al.* 1999). A further potential source within the Musgrave Block is the Mesoproterozoic Alcurra Dyke Swarm, which has been dated as 1070 Ma (Schmidt *et al.* 2006). Furthermore, the eruption of unconformably overlying 1070 Ma volcanic rocks, intrusion of Giles Complex gabbros and a third granulite facies metamorphic event also occurred (White *et al.* 1999) within the Musgrave Block in the Mesoproterozoic.

The Arunta Inlier, central Australia (Figure 1), could be considered to be a second potential source of Mesoproterozoic sediments. Within the Arunta Inlier, an almost complete age spectrum exists from 1800 Ma to 1000 Ma, with age clusters present at ~ 1400 Ma, ~1100 Ma and 400-300 Ma (Collins & Shaw 1995). A ~1150 Ma thermal event in the southern part of the Arunta Inlier (Teapot magmatic event) is recorded by the intrusion of granite and pegmatites (Collins & Shaw 1995). This suggests igneous activity in the region and a possible source of Mesoproterozoic zircons.

Recent SHRIMP zircon work in the Kalkarindji obtained U-Pb SHRIMP ages of 513 ± 12 (2σ) and 508 ± 5 Ma (2σ) (Hanley & Wingate 2000, Macdonald *et al.* 2005) which match U-Pb LA-ICPMS data collected from May River samples and suggest the Kalkarindji province a possible source of Neoproterozoic zircons. The Kalkarindji is a large igneous province (LIP) which covers an extensive area of northern and central Australia (Evins *et al.* 2009).

The wide range of age populations (Figure 9) suggests that the sediment supply is from a variety of sources which is generally expected to occur in detrital sediments, with early igneous activity providing Permian aged zircons (samples 1-02, 3-06 and 5-18). Similar detrital signatures have been reported in conferences from offshore Triassic rocks in the northwest-shelf (Lewis *et al.* 2012).

The nearby Lightjack Formation may be one possible source of the Permian zircons as recent boreholes in the Fitzroy Trough have intersected several Permian tuffs within the 30-300 m thick formation (Mory *et al.* 2012). The formation currently outcrops in the Meda River, north of the May River (Figure 2). The presence of Permian tuffs in the Fitzroy Trough and their proximity to the Erskine Sandstone Formation is evidence of regional Permian volcanism and subsequent erosion. Further to this, as Permian ash-falls are rare in Western Australia (Mory *et al.* 2012), the Lightjack Formation could be concluded as the source of the Permian aged zircons. Unfortunately, as the location of outcrop of the Lightjack Formation in the Triassic is not known, the direction of sediment inflow cannot be defined.

CONCLUSIONS

This report has provided added insight and greater understanding of the provenance of terrestrial Triassic sandstones of the Fitzroy Trough, northern Canning Basin. This analysis of the Triassic Erskine Sandstone Formation at two distinct outcrop locations has enabled observations to be made as to the possible provenance of the formation. Principal findings can be summarised as:

- The wide range of ages collected though U-Pb LA-ICPMS analysis suggests sediment supply to the Erskine Sandstone Formation was from numerous sources;

- Sediment source from the uranium-rich King Leopold Ranges, coupled with the presence of reductants within the Erskine Sandstone Formation could suggest potential sandstone-hosted uranium mineralisation;
- The presence of Permian zircons in the Erskine Range samples, and not in the May River samples, suggests different sources. Further to this, the large amount of Mesoproterozoic zircons in the May River samples, dissimilar to the Erskine Range, further suggests differing sources;
- Sediment sources were predominantly from the King Leopold Ranges to the north, as shown by predominant Palaeoproterozoic ages in all samples;
- Mesoproterozoic sediments may have been sourced from the Musgrave Block or possibly the Arunta Inlier, suggesting a southerly source region, and further suggesting a complex detrital history of the Fitzroy Trough;
- Observations of petroleum well cuttings suggest a silt- fine-grained transition zone between the underlying Blina Shale and the Erskine Sandstone, making boundary identification difficult; and
- The use of a scintillometer in the field gave higher readings in the Blina Shale and lower readings in the Erskine Sandstone Formation. Further measurements at formation boundaries could help delineate Blina/Erskine contact zones.

ACKNOWLEDGEMENTS

"Nothing is difficult, it's just different." Geoff Burdon

First and foremost I would like to thank Joe Potter and Frank Bierlein from Afmeco Pty Ltd for allowing the project to go ahead, and providing financial support. I would also like to thank David Freeman for the field-work support and ideas in the field which have been invaluable.

Secondly I would like to thank Madeleine Iles, Nathanael Pittaway, Holly Feltus, Matthew Fargher and my family for their motivation, support and reviewing throughout the year, as well as Ben Wade and Aoife McFadden for their training, help and expertise at Adelaide Microscopy.

Finally and furthermost, I would like to acknowledge my supervisor Alan Collins for his help and guidance over the year.

REFERENCES

BOTTEN P. 1984. Uranium exploration in the Canning Basin: a case study. *Perth Symposium*, pp. 485-501. Geological Society of Australia/ Petroleum Exploration Society of Australia.

BRETHERTON T. 1998. *Canning Basin EP 129 R3, Millard-1 Well Completion Report. Captial Energy NL*: 1-171.

BROWN S. A., BOSERIO I. M., JACKSON K. S. & SPENCE K. W. 1984. The geological evolution of the Canning Basin, implications for petroleum exploration. *The Canning Basin, W.A. Proceedings of the Geological Society of Australia and Petroleum Exploration Society of Australia Symposium, Perth*, pp. 85-96.

BRUNNSCHWEILER R. O. 1954. Mesozoic Stratigraphy and History of the Canning Desert and Fitzroy Valley, Western Australia. *Geological Society of Australia* **1**, 35-54.

BRUNT D. A. 1990. Miscellaneous uranium deposits in Western Australia. *Geology of the Mineral Deposits of Australia and Papua New Guinea,* Melbourne, pp. 1615-1620. The Australasian Institue of Mining and Metallurgy.

CADMAN S. J., PAIN L., VUCKOVIC V. & LE POIDEVIN S. R. 1993. Canning Basin, W. A. *Bureau of Resource Sciences, Australian Petroleum Acumulations Report 9*.

CAREY S. W. 1976. The expanding earth. *Developments in Geotectonics* **10**.

CATOGRAPHY SERVICES BRANCH S. A. M. D., DEPARTMENT OF MINERALS AND ENERGY, WESTERN AUSTRALIA 1993. *Lennard River 1:250,000 Geological map*. Geological Survey of Western Australia.

COLLINS W. J. & SHAW R. D. 1995. Geochronological constraints on orogenic events in the Arunta Inlier: a review. *Precambrian Research* **71**, 315-346.

DAHLKAMP F. J. 1978. Classification of uranium deposits. *Mineralium Deposita* **13**, 83-104.

ESSO 1982. Booran-1, Well Completion Report. *Esso Australia Limited*.

ESSO 1985. Well completion report Jumjum 1. *Esso Exploration and Production Australia Inc. (unpublished)*.

EVINS L. Z., JOURDAN F. & PHILLIPS D. 2009. The Cambrian Kalkarindji Large Igneous Province: Extent and characteristics based on new 40Ar/39Ar and geochemical data. *Lithos* **110**, 294-304.

GEE R. D. 1987. *Peak Hill, Western Australia - 1:250,000 Geological Seriens - Explanitory notes sheet SG50-8*. Geological Survey of Western Australia.

GOSS R. L. & CRESPIN I. 1955. Final report Fraser River S-1. *West Australian Petroleum Pty Ltd (unpublished)*.

GRIFFIN T. J. & GREY K. 1990. King Leopold and Halls Creek Orogens. *Western Australia Geological Survey Geology and Mineral Resources of Western Australia*.

GRIFFIN W. L., BELOUSOVA E. A., SHEE S. R., PEARSON N. J. & O'REILLY S. Y. 2004. Archean crustal evolution in the northern Yilgarn Craton: U-Pb and Hf-isotope evidence from detrital zircons. *Precambrian Research* **131**, 231-282.

GRIFFIN W. L., J P. W., PEARSON N. J. & O'REILLY S. Y. 2008. *GLITTER: data reduction software for laser ablation ICP-MS. . Laser Ablation ICP-MS in the Earth Sciences: Current Practices and Outstanding Issues.* P. S. **Short Course series 40:** 308-311. Mineralogical Association of Canada.

GUPPY D. J., LINDNER A. W., RATTIGAN J. H., CASEY J. N., CLARKE A. B., BRUNNSCHWEILER R. O., TOWNER R. R., GIBSON D. L. & CROWE R. W. A. 1980. *Derby: Australia 1:250 000 Geological Series*. Bureau of Mineral Resources.

HAINES P. W. & WINGATE M. 2007. Contrasting depositional histories, detrital zircon provenance and hydrocarbon systems: Did the Larapintine Seaway link the Canning and Amadeus basins during the Ordovician? Proceedings of the Central Australian Basins Symposium (CABS), Alice Springs, Northern Territory, 16-18 August, 2005 (unpubl.).

HANLEY L. M. & WINGATE M. T. D. 2000. SHRIMP zircon age for an Early Cambrian dolerite dyke: an intrusive phase of the Antrim Plateau Volcanics of northern Australia. *Australian Journal of Earth Sciences* **47**, 1029-1040.

JACKSON S. E., PEARSON N. J., GRIFFIN W. L. & BELOUSOVA E. A. 2004. The application of laser ablation-inductively coupled plasma-mass spectrometry to in situ U-Pb zircon geochronology. *Chemical Geology* **211**, 47-69.

JAIRETH S., MCKAY A. & LAMBERT I. 2008. Association of large sandstone uranium deposits with hydrocarbons. *Geoscience Australia AUSGEO News* **6**, 89.

KEATS W. 1990. Uranium, *in* Geology and Mineral Resources of Western Australia. *Western Australia Geological Survey, Memoir 3*, 728 - 731.

LAWE A. T. & SMITH R. A. 1989. The Derby Regional Groundwater Investigation 1987. *Geological Survery of Western Australia*.

LEWIS C., SIRCOMBE K., SOUTHGATE P. & ARMSTRONG R. 2012. Insights into provenance pathways on the North West Shelf, Australia(unpubl.).

LONGLEY I. M., BUESSENSCHUETT C., CLYDSDALE L., CUBITT C. J., DAVIS R. C., JOHNSON M. K., MARSHALL N. M., MURRAY A. P., SOMERVILLE R., SPRAY T. B. & THOMPSON N. B. 2004. The North West Shelf of Australia - a Woodside perspective. The Sedimentary Basins of Western Australia 3, Western Australian Basins Symposium Proceedings, Perth (unpubl.).

LUDWIG K. R. 2003. User's Manual for Isoplot 3.00. *Berkeley Geochronological Centre, Special Publication* **4**, 71.

MACDONALD F. A., WINGATE M. T. D. & MITCHELL K. 2005. Geology an age of the Gilkson impact structure, Western Australia *Australian Journal of Earth Sciences* **52**, 641-651.

MCKAY A. D. & MIEZITIS Y. 2001. *Australia's uranium resources, geology and development of deposits* (Vol. Mineral resource Report 1). Geoscience Australia.

MCWHAE J. R. H., PLAYFORD P. E., LINDNER A. W., GLENISTER B. F. & BALME B. E. 1956. The stratigraphy of Western Australia *Journal of Geological Society of Australia: An International Geoscience Journal of the Geological Society of Australia* **4:2**, 1-153.

MORY A. J., CROWLEY J., NICOLL R. S., METCALFE I., MANTLE D., MUNDIL R. & BACKHOUSE J. 2012. Wordian (Middle Permian) U-Pb Ca-IDTIMS isotopic age tie points for the Lightjack Formation, Canning Basin, Western Australia. 34th International Geological Congress, Brisbane (unpubl.).

MUHLING P. C., BRAKEL A. T. & DAVIDSON W. A. 1976. *Mount Egerton 1:250,000 Geological Series - Explanitory notes* (record 1976/12). Geological Survey of Western Australia.

OCCHIPINTI S. A., SWAGER C. P. & PIRAJNO F. 1998. Structural-metamorphic evolution of the Palaerproterozoic Bryah and Padbury Groups during the Capricorn orogeny, Western Australia. *Precambrian Research* **90**, 141-158.

PAGE R. W. 1988. Geochronology of early to middle Proterozoic fold belts in northern Australia: A review. *Precambrian Research* **40/41**, 1-19.

PAYNE J. L., BAROVICH K. M. & HAND M. 2006. Provenance of metasedimentary rocks in the northern Gawler Craton, Australia: Implications for Palaeoproterozoic reconstructions. *Precambrian Research*, 275-291.

PAYNE J. L., FERRIS G., BAROVICH K. M. & HAND M. 2010. Pitfalls of classifying ancient magmatic suits with tectonic discrimination diagrams: An example from the Paleoproterozoic Tunkillia Suite, southern Australia. *Precambrian Research* **177**, 227-240.

PIRAJNO F., ADAMIDES N. G., OCCHIPINTI S., SWAGER C. P. & BAGAS L. 1995. Geology and tectonic evolution of the Early Proterozoic Glengarry Basin, Western Australia. *Geological Survey of Western Australia Annual Revision 1994-1995*, 71-80.

PIRAJNO F. & OCCHIPINTI S. 2000. Three Palaeoproterozoic basins - Yerrida, Bryah and Padbury - Capricorn Orogen, Western Australia. *Australian Journal of Earth Sciences* **47**, 675-688.

REECKMAN A. 1983. *Kora-1, Well Completion Report*. *Esso Australia Limited*.

REEVES F. 1951. Australian Oil Possibilities *American Association of Petroleum Geologists* **35**, 2479-2525.

ROBERTS R. 1985. *East Yeeda No. 1, Well Completion Report*. *Bridge Oil Limited*: 292.

SCHMIDT P. W., WILLIAMS G. E., CAMACHO A. & LEE J. K. W. 2006. Assembly of Proterozoic Australia: Implications of a revised pole for the ~1070 Ma Alcurra Dyke Swarm, central Australia. *Geophysical Journal International* **167**, 626-634.

SKIRROW R. G., JAIRETH S., HUSTON D. L., BASTRAKOV E. N., SCHOFIELD A., VAN DER WIELEN S. E. & BARNICOAT A. C. 2009. Uranium mineral systems: Processes, exploration criteria and a new deposit framework. *Geoscience Australia*.

SLAMA J., KOSLER J., CONDON D. J., CROWLEY J. L., GERDES A., HANCHAR J. M., HORSTWOOD M. S. A., MORRIS G. A., NASDALA L., NORBERG N., SCHALTEGGER U., SCHOENE B., TUBRETT M. N. & WHITEHOUSE M. J. 2008. Plesovice zircon - A new natural reference material for U-Pb and Hf isotopic microanalysis. *Chemical Geology* **249**, 1-35.

SLOAN M. & NEUMANN R. 1984. *Well Completion Report, West Kora-1, Canning Basin Western Australia*. *Volume 1, Esso Australia Limited*.

SMITH R. A. 1992. Explanatory notes on the Derby 1:250 000 hydrogeological sheet. *Geological Survey of Western Australia*.

SPIRAKIS C. S. 1996. the roles of organic matter in the formation of uranium deposits in sedimentary rocks. *Ore Geology Reviews* **11**, 53-69.

TOWNER R. R. 1981. Derby, Western Australia (Second Edition). *1:250 000 Geological Series - Explanitory Notes*.

TYLER I. M. & GRIFFIN T. J. 1990. Structural development of the King Leopold Orogen, Kimberley region, Western Australia. *Australasian Tectonics* **12**, 703-714.

VIELREICHER N. M. & MCNAUGHTON N. J. 2002. SHRIMP U-Pb geochronology of magmatism and thermal events in the Archean Marymia Inlier, central Western Australia. *International Journal of Earth Sciences* **91**, 406-432.

WADE A. 1936. The Geology of the West Kimberley District of Western Australia. *Final Report, Freney Kimberley Oil Company*.

WHITE R. W., CLARKE C. L. & NELSON D. R. 1999. SHRIMP U-Pb zircon dating of Grenville-aged events in the western part of the Musgrave Block, central Australia. *journal of Metamorphic Geology* **17**, 465-481.

WHITEHOUSE M. J. & KEMP A. I. S. 2010. The difficulty of assigning crustal residence, magmatic protelith and metamorphic ages to Lewisian granulites: constraints from combined in situ U-Pb and Lu-Hf isotopes. *Geological Society of London, Special Publications* **335**, 81-101.

YEATES A. N., GIBSON D. L., TOWNER R. R. & CROWE R. W. A. 1984. Regional geology of the onshore Canning Basin, W.A (keynote paper). *The Canning Basin, W.A. Proceedings of the Geological Society of Australia and Petroleum Exploration Society of Australia Symposium, Perth*.

APPENDIX A: SAMPLE LOCATIONS

Derby Field Samples - Honours Project Field Work, Fitzroy Basin - (280512 - 030612)

Sample name	Stop Number	Northing	Easting	Comments
1-01	Stop 1	8028194	635367	Fine grained sandstone (Erskine?)
1-02	Stop 2	8028209	635251	Conglomerate (Erskine?)
1-03	Stop 3	8026251	642181	Blina Shale
1-04	Stop 4	8026369	642278	Conglomerate layer (Meda?)
3-05	Stop 10	8025570	643507	Possible unconformity layer
3-06	Stop 11			Erskine?
3-07	Stop 12			Shale with oxidation
3-08	Stop 15			Erskine or Meda?
3-09	Stop 16	8053634	648703	Hematitic Erskine
4-10	Stop 17	8079114	609109	Rippled sandstone
4-11	Stop 18	8088734	601396	Iron rich sandstone
4-12	Stop 18	8088734	601396	Dark sandstone
4-13	Stop 20	8093267	585105	Fine grained sandstone (Erskine?)
4-14	Stop 20	8093267	585105	Conglomerate (Erskine?)
4-15	Stop 20	8093267	585105	Fine grained sandstone
4-16	Stop 21	8100302	577825	Fine grained sandstone
5-17	Stop 22	8025584	643514	Erskine
5-18	Stop 22	8025561	643505	Fine grained sandstone (Meda?)
5-19	Stop 22	8025544	643505	Bleached oxidised zone
5-20	Stop 22			Possible fluid movement?
5-21	Stop 22			Top of section (Meda?)
6-22	Stop 23	8094242	701624	King Leopold Ranges (fine grained)
6-23	Stop 23	8094242	701624	King Leopold Ranges (coarse grained)
6-24	Stop 24	8104395	722966	Granite outcrop

APPENDIX B: U-PB LA-ICPMS ZIRCON DATA

1-02

Analysis_#	Pb207/U235	1σ	Pb206/U238	1σ	rho	Concordancy	Pb207/Pb206	1σ	Pb206/U238	1σ
10201	2.2261	0.03679	0.19394	0.00244	0.761268	90	1274.3	31.2	1142.7	13.16
10202	1.95888	0.02601	0.18328	0.00206	0.846486	96	1134.4	25.62	1084.9	11.25
10203	0.32653	0.00717	0.04416	0.00056	0.577515	78	355.2	49.71	278.5	3.45
10204	3.59021	0.05752	0.26663	0.0033	0.772513	96	1579.8	29.32	1523.7	16.77
10205	3.73744	0.04886	0.27177	0.00314	0.88379	96	1619.2	22.79	1549.8	15.89
10206	4.41802	0.05884	0.29713	0.00345	0.871822	95	1763.4	22.96	1677	17.12
10207	4.54327	0.05598	0.30551	0.00333	0.884615	97	1764	21.72	1718.6	16.44
10208	4.4669	0.05709	0.29865	0.00336	0.880284	95	1774.3	22.35	1684.6	16.67
10209	4.88731	0.06694	0.32185	0.00382	0.866551	100	1801.7	23.13	1798.8	18.63
10210	5.88271	0.09084	0.35093	0.00435	0.802729	98	1980.1	25.82	1939.1	20.74
10211	0.38534	0.00755	0.04814	0.00059	0.625523	57	532.2	43.32	303.1	3.63
10212	4.74382	0.06925	0.30247	0.00373	0.844763	92	1860.8	24.08	1703.6	18.46
10213	5.01527	0.06134	0.31098	0.00347	0.912321	91	1910.7	20.73	1745.5	17.06
10214	4.81342	0.0765	0.31653	0.00398	0.791153	98	1805.3	27.56	1772.7	19.48
10215	4.70359	0.05885	0.31906	0.00354	0.886776	102	1748	22.08	1785.1	17.3
10216	4.87733	0.06671	0.31802	0.00371	0.852925	98	1820.1	23.53	1780	18.16
10217	0.62328	0.01156	0.08089	0.00097	0.64655	112	447.8	40.74	501.4	5.81
10218	5.13772	0.06219	0.31828	0.00339	0.879914	93	1912.6	21.45	1781.3	16.56
10219	5.52166	0.06994	0.33912	0.00373	0.868359	98	1928	22.25	1882.4	17.96
10220	5.3181	0.07658	0.33694	0.00405	0.834725	100	1872.2	24.42	1871.9	19.55
10221	3.8493	0.04844	0.28583	0.00311	0.86463	103	1580.6	23.06	1620.7	15.61
10222	0.35371	0.00727	0.04879	0.0006	0.59832	99	311	46.9	307.1	3.69
10223	7.05029	0.09527	0.35997	0.00381	0.783266	88	2253.5	23.9	1982	18.06
10224	3.88447	0.05092	0.28013	0.00307	0.836031	97	1635	24.08	1592	15.48
10225	5.11329	0.06593	0.32289	0.00359	0.862298	96	1877.7	22.56	1803.8	17.52
10226	4.98298	0.0615	0.32342	0.00354	0.886851	99	1827.8	21.55	1806.4	17.24
10227	1.93538	0.03614	0.17789	0.00225	0.677344	90	1169.2	36.97	1055.4	12.3
10228	4.69369	0.05718	0.31235	0.00332	0.872503	98	1782.4	22.13	1752.3	16.29
10229	0.47044	0.01369	0.06267	0.00086	0.471563	100	390.1	66.42	391.8	5.21

10231	5.04399	0.06382	0.2882	0.00313	0.858357	79	2055.6	21.88	1632.5	15.68
10232	4.90167	0.06873	0.30991	0.00346	0.796229	93	1875.4	25.06	1740.2	17.01
10233	4.61459	0.07054	0.31002	0.00355	0.749094	99	1765	27.97	1740.8	17.48
10234	5.13773	0.06689	0.33369	0.00343	0.789516	102	1827.5	24.59	1856.2	16.59
10235	0.30189	0.00464	0.0411	0.00043	0.680703	76	341	35.8	259.7	2.67
10236	4.38325	0.06479	0.29564	0.0033	0.75516	95	1758.6	26.94	1669.7	16.41
10237	4.55683	0.06957	0.30599	0.00351	0.751347	97	1766.2	28.35	1720.9	17.32
10238	3.95596	0.07087	0.28415	0.0036	0.707203	98	1641.4	32.57	1612.2	18.06
10239	5.01661	0.0738	0.3279	0.00375	0.777399	101	1815.4	25.94	1828.2	18.22
10240	4.53514	0.05538	0.29988	0.00331	0.903896	94	1794.2	21.37	1690.7	16.42
10241	4.35958	0.05356	0.28687	0.00317	0.899452	90	1803.1	21.5	1625.9	15.88
10242	0.59176	0.01052	0.07553	0.00089	0.662827	97	484	39.64	469.4	5.34
10243	1.9172	0.0304	0.17443	0.00205	0.741185	87	1190.1	31.2	1036.5	11.26
10244	4.30594	0.05107	0.27519	0.003	0.919159	84	1856.1	20.46	1567.1	15.15
10245	1.70719	0.02874	0.15912	0.0019	0.70929	83	1142.4	33.54	951.9	10.57
10246	1.44034	0.01746	0.11265	0.00123	0.90073	46	1482.6	22.16	688.1	7.13
10247	3.05582	0.03735	0.23097	0.00253	0.896194	87	1547.1	22.06	1339.6	13.23
10248	0.33678	0.00521	0.04606	0.00052	0.729773	88	330.1	34.6	290.3	3.22
10249	0.30555	0.00558	0.0391	0.00046	0.644213	52	478.4	40.87	247.3	2.87
10250	4.05734	0.05221	0.26792	0.00297	0.861468	85	1796.9	22.76	1530.2	15.11
10251	4.11795	0.05225	0.27595	0.00304	0.868236	89	1770.1	22.47	1571	15.36
10252	13.04624	0.14959	0.50886	0.0055	0.942643	98	2706.7	18.09	2651.8	23.51
10253	3.29492	0.04096	0.24801	0.00272	0.882236	92	1554.8	22.69	1428.2	14.07
10254	4.93216	0.05935	0.31299	0.00341	0.9054	94	1868.8	21.01	1755.4	16.77
10255	4.04963	0.04768	0.27462	0.00297	0.918551	89	1748.1	20.67	1564.2	15.02
10256	0.40331	0.00707	0.05366	0.00062	0.659114	86	392	39.19	337	3.8
10257	0.33911	0.00508	0.04537	0.00051	0.750375	75	379.5	33.48	286	3.13
10258	0.80254	0.01382	0.09056	0.00106	0.679717	74	750.6	36.59	558.9	6.25
10259	4.32581	0.05201	0.28633	0.0031	0.900483	91	1792.3	21.24	1623.1	15.55
10260	4.27252	0.051	0.29148	0.00315	0.905348	95	1737.1	21.18	1648.9	15.71
10261	1.88585	0.03267	0.17808	0.00211	0.683952	95	1116.2	34.95	1056.4	11.55
10262	4.44274	0.05326	0.29643	0.0032	0.900487	94	1777.7	21.24	1673.6	15.89
10263	4.51578	0.05475	0.29297	0.00317	0.892452	91	1828.8	21.38	1656.3	15.78

10264	0.34149	0.00457	0.04397	0.00048	0.81573	60	464.6	29.31	277.4	2.96
10265	5.08136	0.0623	0.32461	0.00351	0.881936	98	1856.7	21.62	1812.2	17.08

3-06

Analysis_#	**Pb207/U235**	**1σ**	**Pb206/U238**	**1σ**	**rho**	**Concordancy**	**Pb207/Pb206**	**1σ**	**Pb206/U238**	**1σ**
30602	0.38096	0.00632	0.04441	0.00053	0.719378	41	682.2	34.81	280.1	3.26
30603	1.82543	0.02173	0.12084	0.00135	0.938488	41	1792.7	20.13	735.4	7.77
30604	3.4921	0.04343	0.25452	0.00287	0.906686	90	1615.5	21.78	1461.7	14.77
30605	0.35233	0.00502	0.04406	0.0005	0.796474	52	530.1	30.54	277.9	3.11
30606	4.15324	0.05055	0.28377	0.00318	0.920718	93	1734.9	20.96	1610.3	15.95
30607	3.66922	0.04463	0.24154	0.0027	0.919013	77	1802.8	20.82	1394.7	14.01
30608	3.20919	0.03879	0.20949	0.00233	0.92017	67	1818.1	20.65	1226.1	12.42
30609	2.03578	0.0259	0.07009	0.0008	0.89715	15	2911.1	19.97	436.7	4.83
30610	1.11197	0.01379	0.08572	0.00095	0.893656	35	1510.4	22.27	530.2	5.67
30611	1.59959	0.02261	0.15753	0.0018	0.808383	91	1032.3	27.82	943	10.04
30612	0.41664	0.00628	0.05066	0.00058	0.759564	54	591.2	32.1	318.6	3.57
30613	1.53386	0.02078	0.12785	0.00141	0.814064	57	1361.3	25.91	775.6	8.08
30615	0.28634	0.00525	0.03838	0.00045	0.639485	65	375.9	41.57	242.8	2.77
30617	0.64289	0.00853	0.0663	0.00072	0.818477	44	938.6	26.84	413.8	4.37
30618	4.5794	0.05912	0.30772	0.00337	0.848298	98	1765.3	23.19	1729.5	16.63
30619	2.75921	0.03419	0.18295	0.00197	0.868999	61	1789.6	22.14	1083.1	10.75
30620	0.70367	0.01505	0.07343	0.00093	0.592164	50	914.2	44.94	456.8	5.56
30621	5.32092	0.07065	0.35869	0.00396	0.831477	112	1759.5	23.92	1975.9	18.77
30622	4.3082	0.06326	0.28527	0.00327	0.780654	90	1792.1	26.81	1617.8	16.4
30624	0.64464	0.01249	0.07476	0.0009	0.621338	67	693.1	41.85	464.8	5.37
30625	18.34046	0.21462	0.56356	0.00605	0.917393	93	3093.7	17.97	2881.3	24.93
30626	1.28723	0.02408	0.12866	0.00156	0.648158	78	1002.1	38.44	780.2	8.92
30627	2.00937	0.0292	0.16992	0.00192	0.77756	76	1333.2	28.04	1011.7	10.6
30628	0.67678	0.01345	0.07543	0.00092	0.613718	60	777	42.35	468.8	5.51
30629	2.85447	0.03864	0.21592	0.0024	0.82112	82	1545.7	25.14	1260.3	12.72
30630	4.79188	0.06312	0.31954	0.00353	0.838665	100	1779	23.69	1787.5	17.27
30631	4.34681	0.0548	0.29028	0.00315	0.860763	92	1776.4	22.54	1642.9	15.76

30632	4.49641	0.06469	0.29391	0.00336	0.794609	91	1815.4	26.07	1661	16.72
30633	4.92098	0.06556	0.32978	0.00364	0.828495	104	1770	24.05	1837.3	17.67
30634	0.42629	0.00814	0.0565	0.00067	0.621022	88	401	42.81	354.3	4.06
30636	1.01885	0.01472	0.10244	0.00114	0.770261	64	990	29.27	628.7	6.65
30637	4.65363	0.05805	0.29808	0.0031	0.833717	91	1852.1	22.98	1681.8	15.4
30638	0.58976	0.01042	0.07271	0.00081	0.630519	81	561.1	39.43	452.5	4.86
30639	1.26947	0.02542	0.09491	0.00119	0.626155	37	1567.7	39.26	584.5	7.02
30640	0.56557	0.0078	0.07092	0.00074	0.75658	84	523.7	30.93	441.7	4.48
30642	0.50936	0.00728	0.05178	0.00055	0.74318	34	967.8	29.73	325.4	3.39
30643	4.20003	0.06109	0.29117	0.00322	0.760311	96	1708	27.29	1647.4	16.06
30644	3.97086	0.05126	0.21975	0.00232	0.817834	61	2112.6	22.88	1280.6	12.26
30645	0.50493	0.01267	0.05628	0.00073	0.51692	45	777.3	54.22	352.9	4.48
30646	4.46715	0.05803	0.24008	0.00254	0.814434	64	2163.8	22.79	1387.1	13.19
30647	0.46348	0.01334	0.05833	0.0008	0.476511	71	516	64.88	365.5	4.86
30648	2.84107	0.03778	0.18056	0.00192	0.799649	57	1866.5	24.08	1070	10.47
30649	1.34836	0.01974	0.11691	0.00127	0.742012	55	1284.8	28.84	712.8	7.35
30650	3.69102	0.06619	0.27273	0.00354	0.72381	98	1589.7	33.22	1554.7	17.95
30651	0.60275	0.05735	0.06303	0.00163	0.271797	43	909.6	189.06	394.1	9.86
30652	0.33029	0.00542	0.04594	0.00055	0.729571	99	292.3	35.91	289.5	3.42
30653	4.34224	0.06427	0.29644	0.00363	0.827323	96	1736.1	25.92	1673.6	18.03
30654	4.458	0.05918	0.30026	0.00355	0.890627	96	1760.8	22.33	1692.6	17.61
30656	4.17405	0.05535	0.27986	0.00331	0.891923	90	1769	22.27	1590.7	16.68
30657	0.50267	0.00788	0.06648	0.0008	0.767637	102	405.8	33.03	414.9	4.86
30658	0.37073	0.00632	0.05069	0.00062	0.71748	96	331.1	36.97	318.7	3.81
30659	2.79644	0.04931	0.22638	0.00291	0.728996	93	1417.1	32.8	1315.5	15.28
30660	1.44662	0.02428	0.13309	0.00167	0.747613	69	1168.1	32.12	805.5	9.5
30661	0.3539	0.00833	0.04517	0.00061	0.57374	59	484.1	51.71	284.8	3.75
30662	0.65349	0.00944	0.06641	0.00079	0.823494	43	967.8	27.9	414.5	4.8
30663	3.31834	0.04034	0.21207	0.00245	0.950324	67	1855.7	19.86	1239.8	13.05
30664	0.50009	0.00852	0.06636	0.00081	0.716452	104	397.7	36.77	414.2	4.88
30665	4.26727	0.05636	0.2945	0.00347	0.89212	97	1715.6	22.74	1664	17.26
30666	0.48231	0.00878	0.05416	0.00067	0.67956	45	760.4	37.9	340	4.12
30668	3.11995	0.04545	0.23683	0.00284	0.823181	89	1538.4	26.49	1370.2	14.78

30669	0.59504	0.00913	0.07278	0.00086	0.770126	78	577.6	32.23	452.9	5.16
30670	0.42994	0.02833	0.04948	0.00126	0.386458	44	708.5	141.08	311.3	7.71
30671	3.34282	0.04241	0.25373	0.0029	0.900888	95	1538.6	22.43	1457.7	14.9
30672	2.99881	0.03996	0.23248	0.00268	0.865113	90	1498.8	24.07	1347.5	14.02
30673	3.81585	0.05267	0.27325	0.00318	0.843131	95	1647.4	24.75	1557.3	16.12
30674	9.80437	0.12047	0.43957	0.00496	0.918321	95	2473.9	19.56	2348.7	22.23
30675	9.46199	0.11691	0.43123	0.00486	0.912133	94	2446.3	19.83	2311.2	21.91
30676	3.88217	0.04854	0.25273	0.00284	0.898745	80	1822.3	21.61	1452.5	14.61
30678	0.41077	0.00554	0.04526	0.00051	0.835496	36	800.8	27.39	285.3	3.14

3-08

Analysis_#	Pb207/U235	1σ	Pb206/U238	1σ	rho	Concordancy	Pb207/Pb206	1σ	Pb206/U238	1σ
30801R	2.00754	0.03613	0.19678	0.00262	0.739804	111	1041.8	34.51	1158	14.1
30802C	0.42097	0.00902	0.05324	0.00073	0.639926	66	504.9	46.19	334.4	4.45
30803C	2.38411	0.03194	0.15359	0.00192	0.933103	50	1841.9	20.9	921	10.7
30805C	3.47012	0.04904	0.25883	0.00327	0.893979	94	1572.2	23.3	1483.9	16.75
30806R	3.73148	0.04989	0.26928	0.00336	0.93326	94	1633.9	21.21	1537.1	17.05
30807C	4.53315	0.06282	0.30586	0.00385	0.908323	98	1757.7	21.98	1720.3	19.01
30808R	0.36909	0.00624	0.04979	0.00064	0.760301	87	361.6	35.39	313.2	3.95
30809R	0.99626	0.0158	0.11509	0.00148	0.810849	100	701.3	30.67	702.3	8.55
30811C	1.76155	0.02613	0.16951	0.00216	0.859041	94	1078.9	26.45	1009.4	11.91
30810R	0.38528	0.00652	0.05198	0.00067	0.761671	90	361.3	35.27	326.7	4.13
30812R	4.83562	0.06804	0.31434	0.00397	0.897591	97	1825.5	22.11	1762	19.49
30813C	1.90259	0.02541	0.12917	0.00162	0.939061	45	1746.2	20.58	783.1	9.27
30814R	5.62215	0.07553	0.27892	0.00352	0.93939	69	2302	19.63	1585.9	17.74
30815C	4.55764	0.06254	0.30191	0.00382	0.922079	95	1791.1	21.51	1700.8	18.91
30816C	1.14476	0.01806	0.12569	0.00162	0.816979	94	808.5	29.91	763.2	9.28
30817C	4.85161	0.06622	0.3089	0.00389	0.922632	93	1863	21.15	1735.3	19.18
30818C	0.81243	0.01234	0.09909	0.00126	0.837166	104	584.5	29.46	609	7.41
30819R	11.68274	0.15849	0.47845	0.00603	0.929017	96	2626.1	19.36	2520.5	26.29
30820R	3.40065	0.04726	0.25473	0.00321	0.906762	94	1564	22.59	1462.8	16.49
30821R	0.35443	0.00769	0.04763	0.00065	0.62898	81	370	47.28	299.9	4.01
30822C	4.64199	0.06346	0.31293	0.00392	0.916311	100	1759.2	21.47	1755.1	19.25

30823C	1.41572	0.02147	0.14743	0.00188	0.840848	97	918.2	28.03	886.6	10.56
30824R	4.36942	0.06119	0.29532	0.00371	0.897066	95	1754.4	22.31	1668.1	18.48
30825C	3.07084	0.0504	0.24467	0.00321	0.799376	98	1446.8	29.14	1410.9	16.61
30826R	3.47234	0.04694	0.25873	0.00322	0.920637	94	1573.5	21.83	1483.3	16.49
30827R	5.01659	0.06862	0.33377	0.00417	0.91337	104	1782.7	21.67	1856.6	20.16
30828R	7.64334	0.10371	0.39836	0.00497	0.919482	98	2216.6	20.31	2161.5	22.93
30829C	2.06986	0.02817	0.18944	0.00236	0.915365	95	1178.1	23.17	1118.3	12.77
30830C	1.47352	0.02763	0.15089	0.00202	0.713947	95	952.3	36.57	906	11.32
30831C	0.62352	0.00946	0.07702	0.00097	0.830094	86	556.5	29.68	478.3	5.83
30832C	0.37822	0.00639	0.04938	0.00064	0.767136	72	434	34.29	310.7	3.91
30833R	0.77984	0.01171	0.09134	0.00115	0.838466	84	671.4	28.68	563.5	6.82
30834C	1.86603	0.02715	0.1553	0.00196	0.867428	68	1363.9	24.78	930.6	10.93
30835C	0.98705	0.01662	0.11557	0.00149	0.765684	105	672.4	33.27	705	8.64
30836C	5.30302	0.07693	0.33573	0.00424	0.870569	100	1873.1	23.07	1866.1	20.48
30837C	0.60098	0.00938	0.07539	0.00095	0.80736	90	522.6	31.29	468.6	5.71
30838C	2.09228	0.03198	0.19013	0.00241	0.829293	94	1192.3	27.41	1122.1	13.06
30839C	0.71265	0.01607	0.07893	0.0011	0.618032	62	790	46.46	489.7	6.58
30840R	0.32705	0.0087	0.04573	0.00066	0.542547	103	279.4	60.12	288.3	4.04
30841C	1.35426	0.0201	0.12353	0.00155	0.845406	63	1184.9	26.52	750.8	8.87
30842C	1.28859	0.01747	0.09134	0.00112	0.904438	34	1666.4	21.93	563.5	6.62
30843R	3.827	0.05285	0.25223	0.00311	0.892847	81	1800	22.23	1450	16
30844R	1.55864	0.022	0.15446	0.0019	0.871487	91	1018.9	25.49	925.9	10.61
30845R	0.54595	0.00992	0.06977	0.0009	0.709929	90	481.2	38.66	434.7	5.4
30847R	0.55451	0.01111	0.06121	0.00081	0.660477	48	796.6	40.91	383	4.94
30848R	3.35446	0.05193	0.24492	0.00309	0.814964	88	1611.5	26.89	1412.2	15.98
30849R	1.72337	0.02246	0.1658	0.00194	0.897813	92	1080.7	23.75	988.9	10.74
30850R	21.00179	0.26699	0.51383	0.00606	0.927715	77	3453.2	17.76	2673	25.81
30851R	3.38208	0.04983	0.23171	0.00284	0.831891	78	1731.1	25.46	1343.4	14.87
30852R	1.40941	0.0204	0.14579	0.00176	0.83405	94	933.7	27.46	877.3	9.9
30853R	0.45922	0.00861	0.0607	0.00077	0.676581	93	408.9	40.25	379.9	4.68
30855R	0.32881	0.00699	0.04379	0.00058	0.623047	70	392.1	46.37	276.3	3.56
30856R	3.53636	0.04843	0.26733	0.00324	0.884992	99	1548.3	22.9	1527.2	16.46
30857C	3.58265	0.05042	0.26728	0.00327	0.869326	97	1573	23.58	1527	16.62

30858C	1.52087	0.0215	0.09662	0.00119	0.871231	32	1868.2	22.77	594.5	6.97
30859R	3.50093	0.05102	0.26711	0.00331	0.850317	100	1530.6	24.58	1526.1	16.84
30860C	4.91076	0.07057	0.32523	0.00403	0.86227	101	1792.5	23.18	1815.2	19.59
30861C	1.18659	0.01884	0.12483	0.00159	0.802228	84	897.7	30	758.3	9.12
30862R	4.94243	0.06634	0.31321	0.00387	0.920535	94	1871.8	20.8	1756.5	19.01
30863R	2.2718	0.03244	0.20721	0.00259	0.875343	102	1185.6	24.92	1214	13.83
30864C	2.25936	0.03165	0.20806	0.00259	0.888634	104	1166.7	24.3	1218.5	13.81
30865R	3.75721	0.05363	0.2502	0.00314	0.879225	81	1781.8	23.12	1439.5	16.19
30866R	14.66761	0.20542	0.53573	0.00675	0.899652	98	2815	20.21	2765.5	28.34
30867R	0.36943	0.01113	0.05132	0.00078	0.504481	109	295.1	68.21	322.6	4.75
30868R	5.18625	0.07164	0.32095	0.00398	0.897726	94	1914.4	21.61	1794.3	19.42
30869C	5.2594	0.07652	0.35689	0.00449	0.864715	113	1747.3	23.72	1967.4	21.33
30870C	1.88265	0.03108	0.17749	0.00229	0.781538	94	1119.8	30.6	1053.2	12.53
30871R	11.15125	0.15755	0.49908	0.00622	0.882115	105	2477.5	21.02	2609.8	26.76
30872R	3.3825	0.0516	0.22144	0.00282	0.834797	71	1812.7	25.26	1289.5	14.88
30873C	1.92347	0.02939	0.17326	0.00214	0.808353	85	1210.9	28.09	1030.1	11.75
30874R	1.98405	0.03698	0.18701	0.00245	0.702889	99	1121	36.08	1105.2	13.28
30876R	0.66315	0.00937	0.06812	0.00083	0.862334	45	947.1	26.01	424.8	5.01
30878R	10.76974	0.14464	0.46928	0.00571	0.905985	98	2523.1	19.7	2480.4	25.07
30880R	3.68322	0.05767	0.2684	0.00343	0.816186	95	1616.2	26.85	1532.7	17.42
30881R	1.17249	0.01911	0.09906	0.00127	0.7866	46	1335.7	29.28	608.9	7.47
30882R	4.26006	0.06251	0.28739	0.00362	0.858427	93	1758.6	23.82	1628.5	18.12
30883C	25.60653	0.35968	0.59399	0.00741	0.888124	85	3534.9	18.76	3005.6	29.96
30884R	2.48388	0.03875	0.21853	0.0028	0.821308	101	1256.9	27.3	1274.1	14.79

3-09

Analysis_#	Pb207/U235	1σ	Pb206/U238	1σ	rho	Concordancy	Pb207/Pb206	1σ	Pb206/U238	1σ
30901R	0.39987	0.00584	0.05302	0.00059	0.761936	83	400.1	31.32	333	3.63
30902C	4.54887	0.05975	0.30335	0.00338	0.848278	96	1778.5	23.32	1707.9	16.74
30903C	5.20697	0.06451	0.33074	0.00361	0.881005	99	1866.9	21.47	1842	17.48
30904R	2.85737	0.03819	0.17894	0.002	0.836256	56	1892.6	23.51	1061.2	10.94
30905C	8.67197	0.11835	0.45235	0.00514	0.832603	109	2215.3	23.14	2405.7	22.83
30906R	3.53918	0.04612	0.22732	0.00251	0.847324	71	1847	22.89	1320.4	13.16

30907R	3.94003	0.05811	0.26462	0.00305	0.781494	86	1765.9	26.73	1513.4	15.55
30908R	3.92138	0.05384	0.27567	0.00308	0.813758	93	1682.1	24.81	1569.5	15.56
30909R	1.30669	0.01781	0.09045	0.001	0.811148	33	1710.7	24.56	558.2	5.93
30910R	3.74668	0.05236	0.26578	0.00297	0.799615	91	1665.6	25.38	1519.4	15.13
30911R	2.12662	0.02882	0.15295	0.00168	0.810505	56	1640.2	24.57	917.5	9.42
30912R	2.93373	0.0408	0.20329	0.00226	0.799378	70	1709	25.11	1193	12.08
30913C	10.24719	0.144	0.45383	0.00499	0.782437	97	2493.7	23.82	2412.3	22.14
30914R	1.21425	0.02728	0.12005	0.00153	0.567274	71	1022.3	46.68	730.8	8.82
30915R	0.31264	0.00588	0.04167	0.00048	0.61247	68	386.6	42.78	263.2	2.95
30916C	3.82933	0.05584	0.24985	0.00271	0.743819	79	1816.8	26.85	1437.7	13.97
30917C	4.53107	0.06794	0.29624	0.00323	0.727167	92	1812.9	27.72	1672.7	16.07
30918C	9.55735	0.14231	0.40861	0.00442	0.726466	87	2552.4	25.43	2208.5	20.21
30919R	2.37412	0.03751	0.20537	0.00225	0.693428	94	1286.6	31.55	1204.1	12.04
30920R	2.13329	0.0365	0.18343	0.00207	0.659564	84	1298.2	34.27	1085.7	11.26
30921R	4.38226	0.07113	0.27668	0.00305	0.679153	84	1875.6	30.17	1574.6	15.39
30922R	3.34202	0.05513	0.21668	0.00239	0.668652	69	1827.6	30.94	1264.3	12.64
30923C	4.40152	0.07747	0.29236	0.00332	0.645192	93	1783.4	33.35	1653.3	16.55
30924R	4.30159	0.07568	0.29019	0.00326	0.638533	94	1755	33.45	1642.5	16.31
30925R	3.56747	0.0664	0.23941	0.00268	0.60143	78	1766.8	35.12	1383.7	13.94
30926R	0.75711	0.01526	0.08374	0.00096	0.568778	65	792.7	43.54	518.4	5.71
30927R	1.72633	0.03366	0.11916	0.00136	0.585353	42	1715.4	37.02	725.8	7.82
30928R	1.6634	0.03409	0.15058	0.00175	0.567075	75	1199.9	41.67	904.2	9.79
30929R	0.8193	0.0215	0.07348	0.00098	0.508231	38	1218.2	53.48	457.1	5.89
30930R	4.18003	0.08523	0.28267	0.00326	0.56562	92	1753.4	38.45	1604.8	16.38
30931R	0.36535	0.00843	0.04805	0.00058	0.523138	72	418.2	52.37	302.5	3.55
30932R	4.33689	0.09436	0.28458	0.0034	0.549117	89	1808.4	40.83	1614.4	17.05
30933R	3.41814	0.07603	0.24565	0.00295	0.539896	86	1641.5	42.61	1416	15.27
30934C	3.29297	0.07629	0.24319	0.00299	0.530696	88	1590.8	44.69	1403.3	15.5
30935R	2.57627	0.06484	0.20938	0.00271	0.51426	87	1409.8	49.69	1225.5	14.44
30936C	10.34256	0.24391	0.41713	0.00519	0.527587	85	2651.8	40.44	2247.4	23.61
30937C	1.72072	0.04231	0.16115	0.00201	0.507263	85	1133.7	50.22	963.1	11.16
30938R	2.71173	0.06646	0.18553	0.0023	0.505824	63	1732.6	46.36	1097.1	12.53
30939R	3.42228	0.06268	0.2337	0.00255	0.595755	78	1735.8	35.07	1353.8	13.34

30940R	3.17001	0.0672	0.23468	0.00281	0.564835	86	1586.3	41.47	1359	14.66
30941R	2.96267	0.05661	0.22427	0.00247	0.576389	84	1544.5	37.63	1304.4	13.03
30942C	3.77765	0.07385	0.24897	0.00277	0.56912	80	1800.6	37.34	1433.2	14.31
30943C	4.9103	0.09898	0.32681	0.00369	0.560134	102	1782.7	38.63	1822.9	17.94
30944R	4.19752	0.08575	0.27387	0.00309	0.552297	86	1818.9	39	1560.4	15.63
30945R	1.94964	0.04825	0.17604	0.00222	0.509564	87	1205.5	51.03	1045.3	12.17
30946R	3.30702	0.0718	0.2426	0.0028	0.531593	87	1603.3	42.65	1400.2	14.54
30947R	3.64787	0.08005	0.24709	0.00285	0.525615	81	1750.8	42.34	1423.4	14.73
30948R	4.21523	0.09622	0.27751	0.00328	0.517787	88	1802.7	43.84	1578.8	16.54
30949R	0.43174	0.01377	0.05479	0.00076	0.434911	69	497.5	73.43	343.9	4.63
30950R	3.26272	0.07914	0.2394	0.0029	0.49941	86	1603.2	47.85	1383.6	15.11
30951C	4.29489	0.08091	0.28349	0.00302	0.565482	90	1795.2	36.12	1608.9	15.17
30952R	3.17849	0.06325	0.23642	0.0026	0.552649	87	1575.1	39.17	1368.1	13.56
30953R	1.98995	0.04475	0.17662	0.00208	0.523688	85	1237	46.05	1048.5	11.39
30954C	0.62117	0.01328	0.07393	0.00083	0.525134	72	635.5	48.18	459.8	4.95
30955C	2.03025	0.04186	0.12868	0.00143	0.538983	42	1870	39.14	780.3	8.14
30956R	3.4176	0.07501	0.24031	0.00278	0.527078	83	1680.8	42.56	1388.3	14.46
30957R	4.91219	0.10773	0.28037	0.00324	0.526929	77	2057.5	40.67	1593.2	16.3
30958R	4.57207	0.10088	0.298	0.0034	0.517095	92	1820.3	42.04	1681.4	16.9
30960C	2.39916	0.05639	0.15841	0.00187	0.502246	53	1797.3	44.92	947.9	10.43
30961C	4.62834	0.11047	0.29441	0.0035	0.498077	89	1865.2	45.18	1663.5	17.45
30962C	3.58884	0.06906	0.22641	0.00246	0.564634	70	1880.7	36.82	1315.6	12.93
30963R	1.82177	0.03485	0.12158	0.00129	0.554649	42	1778.5	37.07	739.7	7.43
30964R	2.98118	0.06433	0.22697	0.00261	0.532901	86	1534.5	42.85	1318.6	13.73
30965R	4.25338	0.08605	0.28306	0.00308	0.537843	90	1783.7	39	1606.7	15.46
30966R	1.36484	0.03154	0.13115	0.00153	0.504828	73	1082.5	48.68	794.4	8.7
30967R	3.98532	0.08745	0.2717	0.00308	0.516612	89	1739.4	42.28	1549.4	15.59
30969C	3.04318	0.07021	0.22	0.00252	0.496485	79	1631	44.98	1281.9	13.31
30970C	1.63986	0.04286	0.15409	0.00191	0.474257	82	1126.9	54.37	923.8	10.67

4-11

Analysis_#	**Pb207/U235**	**1σ**	**Pb206/U238**	**1σ**	**rho**	**Concordancy**	**Pb207/Pb206**	**1σ**	**Pb206/U238**	**1σ**
41101	4.79486	0.06657	0.3318	0.00418	0.907397	108	1711.8	22.64	1847.1	20.23

41102	5.21986	0.06834	0.33466	0.00415	0.947171	101	1851	20.35	1860.9	20.04
41103	7.91732	0.10332	0.41269	0.00512	0.950692	100	2217.2	19.39	2227.2	23.35
41104	1.87562	0.02704	0.17256	0.00218	0.876303	88	1168.8	25.55	1026.2	11.98
41105	1.68255	0.02577	0.1636	0.00209	0.834097	92	1058	28.46	976.7	11.58
41106	4.80933	0.06553	0.32056	0.00401	0.918078	101	1780.2	21.74	1792.5	19.59
41107	4.64748	0.06346	0.32204	0.00403	0.916458	105	1709.1	21.93	1799.7	19.66
41108	3.63603	0.04889	0.24862	0.0031	0.927327	83	1733.5	21.33	1431.3	15.99
41109	3.29754	0.04763	0.25167	0.00319	0.877544	95	1529.2	24.29	1447.1	16.44
41112	3.96934	0.05767	0.27347	0.00348	0.875866	91	1719.5	23.85	1558.4	17.6
41114	4.77365	0.06324	0.3181	0.00391	0.927837	100	1780.1	21.29	1780.4	19.11
41115	4.51541	0.05936	0.30676	0.00375	0.929899	99	1744.8	21.08	1724.8	18.5
41116	4.38721	0.05728	0.30421	0.0037	0.931566	100	1707.3	21.11	1712.1	18.31
41117	3.54345	0.04743	0.2641	0.00323	0.913708	96	1573.3	22.33	1510.8	16.45
41118	4.62765	0.06422	0.32048	0.00395	0.88815	105	1709.6	23.18	1792.1	19.28
41120	4.57185	0.06196	0.3079	0.00375	0.898674	98	1760.8	22.35	1730.4	18.49
41122	3.27301	0.04784	0.25501	0.00315	0.845103	98	1489.7	25.79	1464.3	16.18
41123	3.73456	0.05181	0.27984	0.0034	0.87578	102	1563.2	23.91	1590.6	17.13
41124	67.71478	2.14785	0.63694	0.02303	0.877253	65	4869.3	56.72	3177	90.68
41125	0.60982	0.01594	0.08195	0.00117	0.546198	137	371.8	58.54	507.7	6.97
41128	5.11845	0.08594	0.33076	0.00423	0.761676	100	1837.2	29.2	1842.1	20.51
41129	5.5763	0.09281	0.35562	0.00452	0.763666	105	1861	28.8	1961.4	21.51
41131	8.69623	0.14226	0.40014	0.00504	0.769958	89	2431.2	26.5	2169.7	23.19
41132	5.26954	0.11129	0.33792	0.00483	0.676784	101	1850.6	38.03	1876.7	23.29
41133	5.91418	0.09928	0.34531	0.00435	0.750435	95	2018.4	28.59	1912.2	20.83
41135	4.50942	0.084	0.30868	0.00405	0.704349	100	1731.4	33.41	1734.2	19.93
41136	7.64691	0.13276	0.36462	0.00461	0.728248	85	2370.1	28.63	2004	21.79
41137	4.62475	0.06251	0.31273	0.00366	0.865865	100	1753.4	22.96	1754.1	17.99
41139	65.73176	3.16822	0.50895	0.02931	0.83695	52	5145.4	82.22	2652.1	125.21
41140	7.06209	0.09455	0.38331	0.00448	0.872971	97	2146.3	21.64	2091.7	20.9
41141	3.46801	0.05451	0.25912	0.00319	0.783238	95	1568.7	28.3	1485.3	16.33
41143	2.66752	0.03612	0.18055	0.00211	0.863068	61	1751.8	22.86	1070	11.54
41145	4.11084	0.05708	0.27541	0.00325	0.849866	89	1770.5	23.59	1568.2	16.42
41146	2.16537	0.0321	0.19969	0.00239	0.807363	101	1163.6	27.68	1173.6	12.85

41147	4.81872	0.06793	0.31078	0.00368	0.839972	95	1839.8	23.73	1744.6	18.1
41148	1.85226	0.0311	0.16814	0.00209	0.740315	84	1194.9	31.97	1001.9	11.54

4-12

Analysis_#	**Pb207/U235**	**1σ**	**Pb206/U238**	**1σ**	**rho**	**Concordancy**	**Pb207/Pb206**	**1σ**	**Pb206/U238**	**1σ**
41201R	2.09017	0.03091	0.19736	0.00237	0.81203	104	1116.4	27.97	1161.1	12.76
41202R	2.11897	0.03623	0.19539	0.00245	0.733365	99	1163.6	33.02	1150.5	13.2
41203R	3.97172	0.05293	0.26831	0.00316	0.883745	87	1755.2	22.39	1532.2	16.07
41204R	4.71903	0.06371	0.30804	0.00365	0.877669	95	1817.7	22.63	1731.1	17.98
41205R	3.30678	0.04475	0.2575	0.00304	0.872386	99	1490.9	23.59	1477	15.6
41207R	3.51261	0.04857	0.24515	0.00292	0.861416	83	1695.4	23.57	1413.4	15.12
41208C	7.90784	1.4858	0.18712	0.02736	0.778204	32	3503.5	317.76	1105.8	148.59
41209C	2.18941	0.03412	0.20057	0.00246	0.787023	100	1176.6	29.27	1178.4	13.19
41210R	2.21546	0.03473	0.20186	0.00248	0.783719	100	1187.3	29.38	1185.3	13.28
41211R	1.88174	0.0296	0.17576	0.00216	0.781271	92	1138.1	29.69	1043.8	11.83
41212R	3.64447	0.05936	0.25718	0.00323	0.771091	88	1675.1	28.9	1475.4	16.58
41213C	2.25008	0.03128	0.21004	0.00246	0.842489	108	1139	26.13	1229	13.1
41214C	4.59878	0.09417	0.31169	0.00432	0.676848	100	1749	38.08	1749	21.25
41215C	2.24235	0.03036	0.20554	0.00238	0.855229	103	1175.1	25.33	1205	12.71
41217C	12.74829	0.16961	0.49704	0.00579	0.875564	96	2707.2	20.99	2601	24.94
41218R	3.95571	0.05261	0.2868	0.00328	0.859906	100	1624.6	23.58	1625.5	16.42
41219R	4.38014	0.05887	0.29814	0.00341	0.850997	97	1741.2	23.6	1682.1	16.93
41220C	3.96732	0.05273	0.27697	0.00314	0.852975	93	1694.7	23.53	1576.1	15.86
41221C	6.6369	0.09038	0.39692	0.00453	0.838085	109	1975.1	23.54	2154.8	20.92
41222C	5.62786	0.07677	0.34121	0.00388	0.833608	97	1950.7	23.74	1892.5	18.64
41223R	2.06962	0.03057	0.18357	0.00211	0.778173	88	1240.1	28.59	1086.5	11.5
41224C	2.07256	0.04931	0.19318	0.00264	0.574399	100	1142.3	48.45	1138.6	14.28
41225R	3.24097	0.05242	0.24053	0.00277	0.712014	88	1581.1	30.26	1389.5	14.42
41226C	3.66945	0.08479	0.24645	0.00344	0.604068	80	1765.6	43.79	1420.1	17.8
41227R	1.95874	0.06519	0.17525	0.00289	0.495491	85	1222.9	67.38	1041	15.85
41228C	5.05022	0.08202	0.32289	0.0037	0.705566	97	1855.2	29.48	1803.8	18.03
41229R	4.53807	0.07749	0.31676	0.00369	0.682215	105	1695	31.8	1773.9	18.09
41230R	0.39814	0.011	0.05372	0.00072	0.485109	94	360.7	63.34	337.3	4.42

41231R	1.78659	0.04489	0.17516	0.00238	0.540776	100	1040.8	52.06	1040.5	13.04
41232C	3.93886	0.07908	0.29938	0.00373	0.620569	110	1536.4	38.71	1688.2	18.49
41233R	4.50825	0.07731	0.30999	0.00355	0.66781	101	1722.7	31.95	1740.6	17.47
41234R	4.86826	0.08592	0.31855	0.00368	0.65456	98	1813.3	32.64	1782.7	18.01
41235C	4.14328	0.07396	0.28046	0.00324	0.647175	91	1751.5	33.28	1593.7	16.32
41236C	2.01859	0.06498	0.1883	0.00297	0.489976	98	1140.6	66.11	1112.2	16.09
41237R	2.73378	0.0549	0.17274	0.00212	0.611131	55	1876.6	37.43	1027.2	11.64
41238R	10.61211	0.2203	0.46019	0.00594	0.62178	96	2530.5	36.26	2440.4	26.22
41239C	12.58097	0.18494	0.43365	0.0047	0.737296	80	2909.1	24.18	2322.2	21.13
41240C	2.46868	0.03905	0.18181	0.00201	0.698911	67	1596	30.13	1076.9	10.98
41241C	3.23596	0.05884	0.24696	0.0029	0.645806	93	1529.2	35.26	1422.8	15.01
41242C	2.10461	0.04416	0.18749	0.00232	0.589729	90	1231.9	42.27	1107.8	12.58
41243R	3.73201	0.0724	0.26445	0.00322	0.627649	91	1667.7	37.12	1512.6	16.4
41244R	2.87614	0.0551	0.21511	0.00257	0.623636	80	1567.2	37.08	1256	13.64
41245C	4.64667	0.11649	0.30788	0.00444	0.575247	97	1790.9	47.76	1730.3	21.86
41246R	4.9279	0.08695	0.33506	0.00383	0.647841	107	1743.7	33.15	1862.9	18.47
41247C	4.37183	0.1518	0.30932	0.00556	0.517676	104	1670.5	66.99	1737.4	27.37
41248R	4.63041	0.08885	0.30832	0.00366	0.618645	97	1782	36.19	1732.4	18.01
41249R	4.26683	0.0815	0.30621	0.00359	0.613794	105	1644.3	36.55	1722	17.69
41250R	2.31532	0.05048	0.20568	0.00254	0.566413	97	1237.6	44.02	1205.7	13.58
41251R	4.49283	0.08935	0.28723	0.00328	0.574208	88	1858.6	37.23	1627.7	16.44
41252R	3.97962	0.08901	0.26167	0.00324	0.553597	83	1807.6	42.35	1498.4	16.55
41253R	1.11684	0.02631	0.10723	0.00132	0.52255	60	1086.1	48.98	656.6	7.68
41254C	3.77877	0.11205	0.26265	0.00399	0.512311	88	1705.6	57.08	1503.4	20.38
41255C	4.9186	0.1096	0.30108	0.00365	0.544054	88	1935.9	41.51	1696.7	18.07
41256C	3.53566	0.10946	0.26062	0.00403	0.499473	94	1596.2	60.32	1493	20.59
41257R	3.68402	0.1007	0.27188	0.00377	0.50729	97	1593.7	53.21	1550.4	19.11
41258C	4.48811	0.10758	0.30085	0.00375	0.520012	96	1771	45.63	1695.5	18.58
41259C	0.58032	0.01973	0.07406	0.00108	0.428924	95	486.1	77.75	460.6	6.48
41260C	3.1673	0.09338	0.23383	0.00339	0.491739	85	1592.3	57.48	1354.5	17.7
41261R	4.84904	0.12537	0.31728	0.00411	0.501027	98	1814.4	48.96	1776.4	20.1
41262C	4.8415	0.12841	0.32965	0.00431	0.492953	105	1741.6	50.56	1836.7	20.92

4-13

Analysis_#	**Pb207/U235**	**1σ**	**Pb206/U238**	**1σ**	**rho**	**Concordancy**	**Pb207/Pb206**	**1σ**	**Pb206/U238**	**1σ**
41302	4.38897	0.0542	0.29063	0.0034	0.947331	92	1791.5	20.11	1644.7	16.99
41303	5.72028	0.07523	0.3079	0.00369	0.911261	80	2160.7	21.08	1730.4	18.17
41304	4.5482	0.06969	0.17285	0.00226	0.853313	37	2749.5	24.9	1027.8	12.4
41305	4.18553	0.05277	0.26967	0.00317	0.932374	84	1841.4	20.48	1539.1	16.12
41306	3.61777	0.04935	0.25082	0.00302	0.88267	84	1707.5	23.21	1442.7	15.55
41307	6.62169	0.08358	0.36723	0.00433	0.934149	96	2108.5	19.82	2016.3	20.4
41308	5.20118	0.07108	0.24393	0.00297	0.890934	59	2398	21.61	1407.1	15.37
41309	9.64045	0.12355	0.31855	0.00378	0.92591	60	2977	18.58	1782.6	18.46
41310	3.95261	0.05139	0.27646	0.00328	0.912529	93	1691.3	21.61	1573.5	16.56
41312	1.62978	0.02223	0.16311	0.00195	0.876483	97	999.2	25.3	974.1	10.82
41313	4.77496	0.06068	0.31265	0.00368	0.926219	97	1812	20.89	1753.7	18.06
41315	4.58104	0.05936	0.29607	0.0035	0.912313	91	1835.6	21.39	1671.8	17.39
41317	4.42551	0.0564	0.30067	0.00352	0.918622	97	1744.5	21.02	1694.6	17.47
41318	5.31082	0.06963	0.32542	0.00385	0.902364	94	1931.5	21.47	1816.2	18.71
41319	2.3691	0.03117	0.17461	0.00206	0.896695	65	1593.9	22.46	1037.4	11.29
41320	9.39327	0.12322	0.33888	0.00402	0.904307	66	2834.4	19.62	1881.3	19.34
41321	2.06391	0.02914	0.18764	0.00224	0.84552	93	1191.1	25.98	1108.6	12.16
41322	2.13196	0.02901	0.16319	0.00193	0.869151	64	1522.8	23.68	974.5	10.72
41323	1.60811	0.02376	0.10534	0.00128	0.822405	36	1810.8	25.52	645.7	7.48
41325	5.12851	0.06813	0.34303	0.00409	0.89752	107	1773.5	22.08	1901.2	19.63
41326	4.17585	0.05485	0.28039	0.00333	0.90417	90	1766.5	21.76	1593.3	16.76
41327	2.60157	0.03673	0.1591	0.00193	0.859215	49	1935.5	23.59	951.8	10.75
41328	4.74974	0.06188	0.30729	0.00364	0.909227	94	1834.1	21.3	1727.3	17.93
41329	3.68773	0.04903	0.24463	0.00291	0.894706	79	1788.5	22.07	1410.7	15.06
41330	0.8133	0.01274	0.08961	0.0011	0.783642	69	801.1	31.12	553.2	6.48
41331	6.7559	0.0901	0.31334	0.00374	0.894982	73	2417	20.68	1757.1	18.34
41332	3.52222	0.04723	0.25445	0.00302	0.885122	90	1631.6	22.73	1461.4	15.54
41334	6.42745	0.09102	0.22071	0.00271	0.86706	44	2914.9	21.63	1285.6	14.33
41335	5.88518	0.08036	0.31584	0.00377	0.874166	82	2166	21.89	1769.4	18.48
41336	4.5488	0.06293	0.29993	0.00359	0.865194	94	1799.4	23.23	1691	17.78
41337	5.13631	0.07889	0.33892	0.00427	0.820276	105	1798.3	26.03	1881.4	20.55

41338	1.71004	0.03042	0.1642	0.00212	0.725788	91	1082.9	34.41	980.1	11.72
41339	0.94435	0.01432	0.08517	0.00105	0.813004	44	1207.4	27.9	526.9	6.23
41341	3.03613	0.04734	0.19482	0.00242	0.796662	62	1848.7	26.86	1147.4	13.07
41342	5.11677	0.08021	0.28938	0.00361	0.795804	79	2074	26.46	1638.4	18.04
41343	0.64142	0.01361	0.07614	0.001	0.618973	74	642.7	45.26	473	6.02
41345	4.26621	0.06432	0.29072	0.00351	0.800808	95	1739.1	26.33	1645.1	17.52
41346	3.3044	0.06735	0.24984	0.00338	0.663758	93	1546.3	38.58	1437.7	17.44
41347	1.75279	0.04056	0.17331	0.00239	0.595945	101	1023.7	47.32	1030.3	13.14
41348	4.2794	0.06661	0.30414	0.00366	0.773127	103	1661.8	28.07	1711.8	18.11
41349	3.70672	0.05236	0.22832	0.00288	0.892974	69	1922.4	21.94	1325.7	15.1
41350	1.32494	0.01979	0.13976	0.00174	0.833521	95	891.3	28.39	843.3	9.83
41351	4.99795	0.06582	0.30057	0.00368	0.929686	86	1964.9	20.68	1694.1	18.26
41352	3.2295	0.04105	0.23666	0.00287	0.954068	85	1604.6	20.37	1369.3	14.97
41353	3.88168	0.05085	0.24606	0.00302	0.936903	76	1870.5	20.58	1418.1	15.61
41354	1.36257	0.01904	0.11272	0.0014	0.88883	50	1375.1	23.96	688.5	8.12
41355	0.7419	0.00978	0.08463	0.00104	0.932214	72	727.6	24.1	523.7	6.18
41356	2.90327	0.038	0.19536	0.00241	0.942508	65	1762.1	20.46	1150.4	12.98
41357	6.22532	0.08247	0.35177	0.00436	0.935607	94	2075.4	20.05	1943	20.78
41358	2.39186	0.03724	0.19012	0.00245	0.827684	77	1451.4	27.2	1122	13.29
41359	4.01494	0.05403	0.25343	0.00316	0.926559	78	1878.2	20.8	1456.1	16.25
41360	6.66483	0.0969	0.31684	0.00409	0.887868	75	2374.8	22.17	1774.3	20
41361	5.11918	0.10035	0.30841	0.0044	0.727792	88	1961.4	33.51	1732.9	21.69
41362	2.00018	0.06106	0.1863	0.00316	0.555631	96	1143	61.09	1101.3	17.16
41363	3.3258	0.08091	0.26006	0.00402	0.635399	101	1482.2	45.82	1490.2	20.59
41364	3.27397	0.09004	0.24853	0.00412	0.602778	93	1538.4	52.09	1430.9	21.26
41365	13.03144	0.25632	0.49855	0.0072	0.734233	95	2738.2	31.19	2607.5	30.98
41366	3.72694	0.07647	0.27136	0.00387	0.695067	96	1616.5	36.84	1547.7	19.61
41367	2.04546	0.06015	0.18041	0.003	0.565478	85	1250.8	57.87	1069.2	16.41
41368	1.74014	0.03593	0.16558	0.00233	0.681514	90	1100.7	39.75	987.7	12.89
41369	2.25313	0.1499	0.16064	0.00524	0.4903	58	1655.7	127.55	960.4	29.12
41370	0.5973	0.01231	0.0566	0.00079	0.677244	32	1109.3	39.65	354.9	4.84

4-14

Analysis_#	Pb207/U235	1σ	Pb206/U238	1σ	rho	Concordancy	Pb207/Pb206	1σ	Pb206/U238	1σ
41401	5.73109	0.0834	0.36686	0.00496	0.929079	109	1852.6	21.63	2014.6	23.39
41403	0.58486	0.00915	0.07348	0.00099	0.861186	88	518.4	29.58	457.1	5.97
41404	17.74779	0.25053	0.4379	0.00585	0.94638	68	3438.2	17.78	2341.2	26.22
41405	4.43428	0.06458	0.30717	0.00411	0.91873	101	1708.5	22.2	1726.8	20.28
41406	10.14313	0.14514	0.47935	0.00638	0.93015	106	2384.4	20.01	2524.5	27.82
41407	0.56889	0.01038	0.07423	0.00102	0.753098	106	434.7	36.53	461.6	6.14
41408	7.16254	0.10326	0.39732	0.00527	0.920037	102	2107.6	20.96	2156.7	24.32
41409	0.74911	0.01546	0.09225	0.00131	0.688083	101	562.6	42.32	568.9	7.72
41410	0.73139	0.01519	0.08953	0.00127	0.683009	96	575.9	42.59	552.7	7.51
41411	0.60017	0.0109	0.07313	0.001	0.752926	78	585.9	36.08	455	6.02
41412	5.57268	0.08321	0.35487	0.00471	0.888874	105	1862.2	23.03	1957.8	22.4
41413	4.91309	0.0689	0.3263	0.00428	0.935324	102	1786.3	21.03	1820.4	20.81
41414	4.72725	0.06742	0.3237	0.00426	0.922756	104	1730.4	21.83	1807.8	20.74
41415	24.94882	0.36483	0.4819	0.00666	0.945098	66	3813.9	19.43	2535.5	28.96
41416	0.94076	0.01522	0.08188	0.0011	0.830384	40	1277	28.3	507.3	6.56
41417	5.33155	0.07564	0.33921	0.00443	0.920528	101	1864.3	21.54	1882.9	21.34
41418	4.45104	0.06213	0.30433	0.00395	0.929849	99	1733.3	21.37	1712.7	19.52
41419	3.78838	0.05304	0.27562	0.00357	0.92514	97	1618.6	21.86	1569.2	18.04
41420	9.39365	0.1313	0.43115	0.00559	0.927584	95	2434.8	19.97	2310.9	25.19
41421	11.47273	0.20198	0.24108	0.00383	0.902394	38	3685.9	27.3	1392.3	19.88
41422	4.52857	0.0642	0.30912	0.00399	0.910483	100	1736.3	22.21	1736.4	19.67
41423	4.33641	0.06171	0.30253	0.0039	0.905881	100	1696.2	22.53	1703.9	19.32
41424	0.48164	0.01063	0.06504	0.00091	0.633943	113	359	48.1	406.2	5.51
41425	7.29964	0.10376	0.4125	0.00531	0.905612	107	2075.7	21.66	2226.3	24.23
41426	3.60331	0.0512	0.2797	0.0036	0.90582	106	1497	23.2	1589.9	18.11
41427	2.05952	0.03251	0.1943	0.00254	0.828152	102	1118.4	28.42	1144.6	13.73
41428	0.66042	0.01208	0.0846	0.00113	0.730233	110	476.5	38.25	523.5	6.69
41429	1.46338	0.02073	0.14129	0.0018	0.89933	79	1072.1	24.62	851.9	10.15
41430	0.66879	0.01039	0.08452	0.00109	0.830121	103	506.6	30.49	523	6.46
41431	2.17929	0.03451	0.20361	0.00265	0.821896	105	1137.8	28.62	1194.7	14.17
41432	4.51644	0.06694	0.30396	0.00391	0.867902	97	1762.5	24.12	1710.9	19.32

41433	0.80008	0.0121	0.09631	0.00123	0.844465	97	613.3	29.2	592.7	7.21
41434	1.10715	0.01629	0.10125	0.00128	0.859212	53	1180.4	25.87	621.8	7.52
41435	1.55536	0.0239	0.16204	0.00207	0.831345	105	917.9	28.56	968.1	11.47
41436	0.51742	0.00901	0.06662	0.00081	0.69823	89	465	37.84	415.7	4.9
41437	2.08151	0.03157	0.19043	0.00228	0.789411	95	1179.3	28.62	1123.7	12.37
41438	0.4204	0.01203	0.05457	0.00078	0.499503	77	447.2	63.75	342.5	4.78
41439	1.60302	0.02567	0.16155	0.00197	0.761504	98	985.4	31.18	965.4	10.93
41440	10.65357	0.15739	0.47328	0.00579	0.828092	100	2490.1	23.42	2497.9	25.35
41441	4.74068	0.08107	0.3193	0.0041	0.750871	101	1761	30.18	1786.3	20.05
41442	2.02424	0.05793	0.18431	0.00292	0.553595	92	1189	57.14	1090.5	15.9
41443	7.50423	0.1148	0.38275	0.00473	0.807812	93	2254.6	24.71	2089.1	22.03
41444	4.98858	0.07594	0.32725	0.004	0.802947	101	1809.2	25.66	1825	19.45
41445	2.37178	0.07613	0.19205	0.00335	0.543437	80	1417.1	62.28	1132.5	18.14
41446	2.20485	0.04782	0.20314	0.00282	0.640064	102	1165.8	42.2	1192.2	15.09
41447	4.3911	0.07733	0.31798	0.00413	0.737523	109	1627.7	31.03	1779.9	20.19
41448	4.35945	0.07575	0.30079	0.00389	0.744278	99	1717.1	30.05	1695.2	19.26
41449	6.64855	0.09759	0.3856	0.00479	0.846292	104	2030.1	24.11	2102.4	22.31
41450	4.92935	0.08057	0.32515	0.00418	0.786518	101	1799.2	28.49	1814.8	20.35
41452	4.43693	0.07087	0.3069	0.00385	0.785388	101	1712.1	28.14	1725.4	19.01
41453	0.81554	0.02906	0.09946	0.00165	0.46557	105	584.7	78.08	611.3	9.67
41454	5.60703	0.09865	0.33172	0.00434	0.743625	93	1994.5	30.83	1846.7	21
41455	4.60562	0.07913	0.31444	0.004	0.740405	102	1735.9	30.9	1762.5	19.6
41456	1.11849	0.02174	0.11338	0.00146	0.662505	71	973.1	39.56	692.3	8.47
41457	6.79646	0.12335	0.38333	0.00484	0.695691	101	2068.4	31.39	2091.8	22.55
41458	4.63191	0.08216	0.30307	0.00373	0.69385	95	1803.4	31.56	1706.5	18.45
41459	7.00448	0.12928	0.35232	0.00445	0.684333	86	2269.7	31.42	1945.7	21.19
41460	2.1401	0.09159	0.19469	0.00393	0.471666	97	1181.5	86.17	1146.7	21.23
41461	4.40417	0.0844	0.29022	0.00366	0.658075	92	1793.3	34.68	1642.6	18.27
41462	3.31722	0.06382	0.22741	0.00285	0.651408	77	1721.9	35.18	1320.9	14.95
41463	4.2104	0.09313	0.28945	0.00393	0.613837	95	1717.8	41.07	1638.8	19.66
41464	4.11602	0.08464	0.27805	0.00358	0.626126	90	1750.9	37.8	1581.5	18.03
41465	4.58383	0.10273	0.30861	0.00418	0.604362	99	1758	41.52	1733.8	20.59
41466	4.22404	0.09455	0.28271	0.00379	0.598914	91	1769.7	41.58	1605	19.06

41467	0.59138	0.02543	0.0752	0.00135	0.417481	95	490.6	96.62	467.4	8.08
41468	1.52587	0.03278	0.10411	0.00133	0.594659	37	1736.4	40	638.5	7.75
41469	5.18623	0.12327	0.32894	0.00452	0.578118	98	1870.2	43.92	1833.2	21.93
41470	5.46748	0.0973	0.35192	0.00448	0.715333	106	1841.9	32.18	1943.8	21.37
41471	6.13448	0.11539	0.32753	0.00435	0.70607	84	2173.7	33.21	1826.4	21.15
41472	8.49286	0.16577	0.38851	0.00539	0.710779	87	2439.1	33.79	2115.9	25.04
41473	2.36679	0.04083	0.12497	0.00155	0.718963	35	2193	30.48	759.1	8.86
41474	2.00526	0.0569	0.19057	0.00292	0.539991	102	1102	58.24	1124.5	15.79
41475	3.70821	0.08068	0.25876	0.00357	0.634117	88	1694.4	41.36	1483.5	18.29
41476	0.85961	0.02271	0.09699	0.00136	0.530758	80	749.5	57.3	596.8	7.99
41477	4.18196	0.07004	0.28915	0.00341	0.70415	96	1711.4	31.59	1637.3	17.06
41478	5.03357	0.08561	0.31854	0.00377	0.695871	95	1872.8	31.66	1782.6	18.45
41479	0.48795	0.01978	0.06205	0.00107	0.425394	79	491.1	91.92	388.1	6.51
41480	1.88438	0.04311	0.17621	0.00234	0.580465	92	1134.7	47.71	1046.2	12.84
41481	3.29216	0.06372	0.24899	0.00308	0.639108	93	1545.2	38.19	1433.3	15.92

5-18

Analysis_#	**Pb207/U235**	**1σ**	**Pb206/U238**	**1σ**	**rho**	**Concordancy**	**Pb207/Pb206**	**1σ**	**Pb206/U238**	**1σ**
51801R	4.23745	0.05486	0.29735	0.00346	0.898787	100	1684.9	22.13	1678.2	17.2
51802C	0.68165	0.0118	0.06887	0.00085	0.712965	44	979.5	34.62	429.3	5.15
51804R	0.66012	0.01245	0.08223	0.00103	0.664141	95	536.8	41.17	509.4	6.13
51805R	7.46958	0.09686	0.2695	0.00313	0.895648	54	2833.9	19.61	1538.3	15.91
51806R	5.0454	0.06754	0.32351	0.00378	0.872848	98	1849.3	22.6	1806.8	18.41
51807R	2.49998	0.03466	0.18094	0.00213	0.849089	66	1627.1	24.29	1072.1	11.62
51808C	0.58097	0.02416	0.06636	0.0012	0.434842	57	723.9	89.34	414.2	7.24
51809R	1.77462	0.02485	0.10848	0.00128	0.842635	34	1935	23.71	663.9	7.43
51810R	0.5233	0.00965	0.05701	0.00071	0.675353	43	823.3	37.96	357.4	4.35
51811C	3.55965	0.05249	0.26846	0.0032	0.808353	99	1549.9	26.39	1533	16.26
51812C	4.99896	0.07254	0.32196	0.00382	0.817643	98	1840.8	24.95	1799.3	18.63
51813R	0.64361	0.01306	0.07463	0.00094	0.620718	67	692.2	43.3	464	5.62
51814C	4.61656	0.06413	0.31418	0.00362	0.829444	101	1741	24.43	1761.3	17.77
51815R	4.4689	0.06054	0.29578	0.00337	0.841045	93	1791.9	23.74	1670.4	16.76
51817C	4.63901	0.06911	0.31404	0.00369	0.788725	101	1751	26.69	1760.6	18.08

51818C	4.65119	0.06533	0.30482	0.00348	0.812807	95	1810.2	24.85	1715.2	17.22
51819R	3.19524	0.04399	0.23577	0.00266	0.819488	86	1591.8	24.99	1364.7	13.86
51820R	0.37362	0.00655	0.04158	0.00049	0.672203	34	779.9	36.88	262.6	3.05
51821R	0.62093	0.01362	0.07464	0.00095	0.580253	75	615.7	47.89	464.1	5.68
51822C	3.90381	0.06369	0.28627	0.00341	0.730123	101	1603.8	30.42	1622.9	17.11
51823R	0.43353	0.00772	0.05833	0.00068	0.654665	99	367.4	40.24	365.4	4.16
51824R	2.81195	0.04037	0.19007	0.00214	0.78424	64	1754.4	25.95	1121.8	11.57
51825C	0.99657	0.01845	0.11675	0.0014	0.647713	106	673	39.7	711.8	8.07
51826C	8.10805	0.13014	0.36168	0.00422	0.726932	80	2484.2	26.99	1990.1	19.98
51827C	0.48816	0.01058	0.06258	0.00078	0.57509	82	476.2	48.88	391.3	4.74
51828C	4.70991	0.07961	0.31676	0.00372	0.694796	101	1764.7	30.91	1773.9	18.23
51829C	4.47025	0.07371	0.29556	0.00341	0.699704	93	1795.7	30.02	1669.3	16.96
51830C	1.19439	0.02704	0.1254	0.00162	0.570633	84	902.7	47.47	761.6	9.3
51831C	0.87852	0.01886	0.08918	0.00113	0.59023	57	971.8	44.57	550.7	6.67
51832C	1.90521	0.03527	0.16408	0.00196	0.645265	75	1298.8	36.43	979.4	10.85
51833C	4.97557	0.08961	0.33265	0.00392	0.654312	104	1775.3	33.25	1851.2	18.96
51834C	0.56876	0.01202	0.07048	0.00087	0.584088	80	551.2	46.85	439	5.23
51835C	4.24474	0.0824	0.19647	0.00241	0.631895	48	2421.5	33.66	1156.3	13
51836C	5.0166	0.09999	0.29279	0.00361	0.618591	82	2019.5	36.1	1655.5	18
51837C	0.40752	0.00976	0.05393	0.00069	0.534217	83	405.6	53.95	338.6	4.23
51838C	0.34832	0.00975	0.04674	0.00064	0.489176	79	374.4	64.07	294.5	3.92
51839C	5.14093	0.10703	0.32272	0.00399	0.593859	95	1889.4	38.4	1803	19.42
51840C	4.55549	0.08394	0.30796	0.00366	0.64499	99	1755.3	34.19	1730.7	18.05
51841C	4.54334	0.0846	0.30827	0.00366	0.637609	99	1748.3	34.69	1732.2	18.05
51842C	1.49752	0.02933	0.15131	0.00182	0.614136	93	980.9	40.79	908.3	10.16
51843R	4.86541	0.09184	0.32628	0.00385	0.625112	103	1769.2	35.42	1820.3	18.71
51844R	0.38923	0.00883	0.05234	0.00065	0.547426	89	368.8	52.45	328.9	3.99
51845R	0.36266	0.01006	0.04736	0.00064	0.487158	69	434.3	63.23	298.3	3.95
51846R	0.30975	0.00763	0.04361	0.00056	0.521301	104	264	58.26	275.2	3.43
51847R	3.42124	0.07146	0.25526	0.0031	0.581433	93	1571.3	40.73	1465.6	15.94
51848R	2.38764	0.0511	0.21946	0.00267	0.568465	109	1169.8	44.22	1279	14.13
51849R	0.77052	0.02314	0.09436	0.00134	0.472865	101	575.2	67.54	581.3	7.88
51850R	0.28986	0.00731	0.04001	0.00051	0.505443	82	309.2	59.7	252.9	3.17

51852R	0.42454	0.01035	0.05164	0.00065	0.516304	55	589.7	55.73	324.6	3.99
51853R	3.8248	0.06055	0.25892	0.00281	0.685544	85	1751.5	29.45	1484.3	14.38
51854R	0.36593	0.00793	0.04932	0.00059	0.552019	85	363.3	49.9	310.3	3.59
51856R	4.20465	0.07127	0.27967	0.00314	0.662379	89	1783.4	31.37	1589.7	15.82
51857R	0.31379	0.00561	0.04168	0.00047	0.630734	66	396	40.23	263.2	2.9
51858R	6.85856	0.11552	0.32835	0.00366	0.661789	77	2362.8	28.94	1830.4	17.79
51859C	1.47971	0.02649	0.138	0.00157	0.6355	73	1140.8	35.83	833.4	8.91
51860C	3.64594	0.08565	0.2742	0.00372	0.577508	100	1556.1	44.96	1562.1	18.81
51861R	1.30749	0.025	0.13974	0.00163	0.61005	98	864.1	39.79	843.2	9.24
51863R	4.51799	0.08411	0.29169	0.0034	0.626116	90	1837.3	33.57	1650	16.97
51864R	1.02545	0.02039	0.11846	0.00141	0.598611	103	700.6	42.14	721.7	8.12

APPENDIX C: ERSKINE SANDSTONE FORMATION OUTCROP LOCATIONS

Table 1. Locations and comments of outcrop of the Erskine Sandstone Formation, with stop numbers relating to stop locations in the field.

Unit	Outcrop Location		Comments
	Northing (mN)	Easting (mE)	
Erskine Sandstone Formation	8028194	635367	[Stop 1] Limited bedding due to it being highly ferruginised and probably flooded by iron rich fluids, weak to moderately silicified, predominantly quartz, poorly sorted bands with larger clasts being 1-5 mm and finer being <1 mm, sub-angular to sub-rounded grains, conglomeritic layer present 10-20 mm clasts.
Erskine Sandstone Formation	8028209	635251	[Stop 2] Conglomeritic layers comprising of sub-angular quartz and ranges from 3 mm to 20 mm.
Erskine Sandstone Formation	8025570	643507	[Stop 11] Banded sandstone, layers of bleached and red sandstone, layers range from 1-10 mm, medium to fine grained, massive texture, no great change in the grain size, cross-bedding is seen on a relatively weathered surface
Erskine Sandstone Formation	8053634	648703	[Stop 16] Highly ferruginised, hematite replacement and intensely iron altered, very oxidised.
Erskine Sandstone Formation	8093267	585105	[Stop 20] Mostly fine-grained with some slight layering present, fine grained layers are 20 – 300 mm thick, mud lenses are present in fine grained sections and also in the conglomeritic areas, conglomerate caps the outcrop and is poorly sorted suggesting a fluvial environment.
Erskine Sandstone Formation	8025584	643514	[Stop 22] Proportionally more oxidised layers and less bleached layers, very fine to fine grained.

APPENDIX D: PETROLEUM WELL HOLE CUTTINGS LOGS

Table 1. Geological log of the East Yeeda 1 hole. The upper section was targeted as it comprised mainly of the Erskine Sandstone Formation.

Sample (m)	Comments
45	Predominantly quartz, close to 100%
	Clear to frosted quartz, pink to red Fe staining,
	Coarse to very coarse grained
	Moderate sorting
	Angular to sub-angular
	Small v.fg clasts that are hard and orange when broken
	Stained quartz gives the overall indication that it is orange/red sandstone
	Quartz 95%, clasts 5%
	Oxidised
50	Angular to sub-angular
	Clear to frosted quartz, pink to red Fe staining
	Poorly sorted
	Same clasts as seen in 45 m
	Overall orange to black colour
	50% quartz, 50% clasts
	Oxidised
55	Predominantly angular, partly sub-round
	Quartz ranges from clear to Fe stained, pink-red
	Poorly sorted
	Medium to coarse grained
	Larger quartz grains are mostly clear/white
	Fine grained clasts present, made of f.g sediments
	Some coarse grains present that look like quartzite
	Orange-black in colour
	60% quartz, 20% quartzite, 20% fg clasts
	Oxidised
60	Less quartz than seen in previous sections
	Quartz is clear to stained red
	Sub-angular to sub-rounded
	Poorly sorted
	Trace mica
	Concrete contamination or a fg felsic volcanic rock
	40% quartz, 40% fg clasts, 20% contamination, trace mica
	Oxidised
65	Trace mica
	Pitted clasts present, infill is white
	Poorly sorted
	Medium to coarse grained
	Quartz clear to frosted to pink
	Some coarse clasts which break into red fg sediments
	Larger concrete (felsic) clasts present

	Quartz grains are round when not fractured
	60% clasts, 30% quartz, 10% contamination, trace mica
70	Very coarse to small pebbles in size
	Poorly sorted
	Same composition as 65 m but much coarser grained
	Slightly less quartz present
	Sub-rounded
	Clasts are well cemented and contain mica
	Quartz grains are round when not shattered
	70% clasts, 20% quartz, 10% contamination, trace mica
	Oxidised
75	Trace mica
	Poorly sorted
	Medium to coarse grained
	Quartz clear to frosted to pink
	Some coarse clasts which break into red fg sediments
	Larger concrete clasts present
	Quartz grains are round when not fractured
	60% clasts, 30% quartz, 10% contamination, trace mica
	Oxidised
80	Quartz grains are sub-angular to sub-round
	Quartz is clear to red/orange
	Quartz is medium to coarse grained
	Trace mica
	Other clasts are angular to sub-rounded
	Overall brown in colour
	70% clasts, 20% quartz, 10% contamination, trace mica
	Oxidised
85	Trace lignite/coal (bitumonous/shiney)
	Same as 80m
	55% clasts, 40% quartz, 5% concrete contamination
	Oxidised
90	Medium to coarse grained
	Moderate sorting
	Sub-angular to sub-rounded
	Black clasts present, hard to break but are red-brown on the inside and are mostly magnetic
	These black clasts could be less weathered versions of the clasts seen previously in the hole
	70% clasts, 20% quartz, 10% contamination
	Oxidised
165	Large amount of concrete contamination
230	Blina Shale
	Grey in colour
	Fine grained
	Some laminar clasts
	Trace amounts of the red magnetic clasts
	Poorly sorted clasts but they break down to the same fg size

Table 2. Geological log of the West Kora 1 hole. The upper section was targeted as it comprised mainly of the Erskine Sandstone Formation.

Sample (m)	Comments
30-40	Almost completely quartz
	Clear, slightly Fe stained
	Medium grained
	Sub-angular to sub-rounded
	Moderate to well sorted
	Trace mica
	Some clasts that are hard and red, slightly magnetic
	90% quartz, 10% clasts, trace mica
	Oxidised
	Erskine Sandstone Formation
40-50	Fine grained
	Well sorted
	100% silt, trace mica
50-60	Very fine grained quartz
	Quartz are sub-rounded
	Quartz are Fe stained
	95% silt, 5% quartz, trace mica
	Well sorted
	Oxidised
60-70	Quartz rich sand
	Slightly more mica
	Hard clasts present
	Poorly sorted
	Sub-angular
	Some well rounded quartz
	Fine to coarse grained
	Brown in colour
	80% clasts, 19% quartz, 1% mica
70-80	As above
80-90	Large amount of clasts, medium grained
	Sub-rounded
	Well sorted
	Some quartz grains are sub-rounded, clear to frosted Fe stained
	Some clasts are magnetic
	Trace mica
	Oxidised
90-100	As above
	Some coarser round white to frosted quartz grains
	Well sorted
	Oxidised
100-110	Moderate to well sorted
	Sub-angular to sub-rounded
	Quartz is predominantly clear, some frosted and Fe stained
	Very thin, pitted clasts seen

	50% quartz, 45% clasts, 5% mica
110-120	Sub-angular to sub-rounded
	Moderate sorting
	Quartz is clear to frosted with Fe staining
	Brown/black in colour
	60% clasts (mildly magnetic), 40% quartz, Trace mica
	Oxidised
120-130	Fine grained
	Clasts are slightly coarser than the quartz
	Quartz is mostly clear-frosted
	Clasts are mostly magnetic
	65% quartz, 35% clasts, trace mica

Table 3. Geological log of the Booran 1 hole. This section was targeted as it comprised mainly of the Erskine Sandstone Formation.

Sample (m)	Comments
235-240	Poorly sorted
	Angular to sub-angular
	Quartz is clear to Fe stained
	Small maroon/brown clasts
	Silty clasts present
	50% quartz, 50% clasts, trace mica
240-245	Little to no quartz, mostly very fg
	Mostly clasts comprised of fg sediments
	Some magnetic clasts
	Moderate sorting
	Sub-rounded
	~1% mica
	Oxidised
245-250	Poorly sorted
	As above
	Very fine to coarse grained
	The coarse grains are the sediment clasts
	Oxidised
250-255	As above
	Limited coarse grains of quartzite
	Some magnetic grains
	Boundary between Erskine Sandstone Formation and Blina Shale
255-260	Clasts of fine grained sediments
	Looks shaley
	Some magnetic grains
	Clasts present which look like the harder ones seen earlier however these are now soft
	Trace mica
260-265	Not as shaley as 255-260m
	Contains predominantly coarse grained clasts
	Quartz is present as fg clear to frosted, some with Fe staining

APPENDIX E: GAMMA-RAY DATA

Table 1. Gamma-ray Spectrometer measurements taken of the petroleum well-hole cutting samples

Bag #	Dk ($nSvh^{-1}$)	K %	U ppm	Th ppm	Reading #	Comment	Count length
BACKGROUND	233.2	2.6	12.7	33.2	1088	Taken of air	300 Second Count
EAST YEEDA 1							
Bag #	Dk ($nSvh^{-1}$)	K %	U ppm	Th ppm	Reading #	Comment	Count length
45	237.5	2.5	12.1	36.2	1073	In sample bag- Sand	300 Second Count
45	262.9	2.6	13.2	41.2	1074	On sheet - Sand	300 Second Count
50	242.0	2.7	13.6	33.7	1075	On sheet - Sand	300 Second Count
55	253.0	3.0	10.9	41.0	1076	On sheet - Sand	300 Second Count
60	253.3	2.8	11.5	41.0	1077	On sheet - Sand	300 Second Count
65	247.1	2.4	13.3	37.2	1078	On sheet - Sand	300 Second Count
70	244.7	2.9	13.3	34.3	1079	On sheet - Sand	300 Second Count
75	261.0	3.2	8.8	46.9	1080	On sheet - Sand	300 Second Count
80	256.9	2.9	12.1	40.3	1081	On sheet - Sand	300 Second Count
160	264.0	2.9	10.4	45.9	1082	On sheet - Sand/ cement	300 Second Count
245	252.1	2.8	15.6	32.2	1083	On sheet - Silt	300 Second Count
265	237.3	3.0	11.9	34.5	1084	On sheet - Silt	300 Second Count
Whole box	276.5	3.1	12.4	44.7	1094		300 Second Count
WEST KORA 1							
Bag #	Dk ($nSvh^{-1}$)	K %	U ppm	Th ppm	Reading #	Comment	Count length
30-40	253.6	2.6	13.9	37.0		Fine-medium grained sand	300 Second Count
40-50	269.2	2.7	15.0	39.3	1085	f.g sand	300 Second Count

50-60	255.2	2.7	14.6	36.0	1086	f.g sand	300 Second Count
60-70	241.2	2.8	12.1	36.2	1089	f.g sand	300 Second Count
70-80	237.7	2.5	11.2	37.9	1090	f.g sand	300 Second Count
80-90	244.3	2.4	14.9	33.3	1091	f.g sand	300 Second Count
90-100	241.7	2.9	10.9	38.1	1092	f.g sand	300 Second Count
190-200	241.7	2.9	12.6	34.8	1093	silt	300 Second Count

KORA 1

Bag #	Dk ($nSvh^{-1}$)	K %	U ppm	Th ppm	Reading #	Comment	Count length
160-165	239.4	2.5	12.6	35.8	1097		300 Second Count

BOORAN 1

Bag #	Dk ($nSvh^{-1}$)	K %	U ppm	Th ppm	Reading #	Comment	Count length
165-170	246.7	2.4	12.5	39.0	1098	Sand	300 Second Count
170-175	256.9	2.5	14.5	37.4	1099	Sand	300 Second Count
175-180						No Sample	
180-185						No Sample	
185-190						No Sample	
190-195	229.3	2.3	12.2	34.4	1104	Sand	300 Second Count
195-200	231.5	2.3	14.2	31.2	1101	Sand	300 Second Count
200-205	238.3	2.4	14.1	33.2	1102	Silt	300 Second Count
205-210	227.7	2.6	12.5	32.1	1103	Silt	300 Second Count
210-215	242.4	2.8	11.4	38.0	1105	Sand	300 Second Count
215-220	232.4	2.3	137.0	32.7	1106	Sand	300 Second Count
220-225	252.0	2.5	14.1	36.6	1107	Sand/Silt	300 Second Count

225-230	229.0	2.4	12.8	32.6	1108	Sand/Silt	300 Second Count
230-235	223.9	2.5	13.8	28.9	1109	Sand/Silt	300 Second Count
235-240	226.6	2.6	11.6	33.3	1110	Sand/Silt	300 Second Count
240-245	246.7	2.4	12.3	39.0	1111	Sand/Silt	300 Second Count
245-250	243.9	2.2	15.9	32.0	1112	Sand/Silt	300 Second Count
250-255	249.3	2.7	13.8	35.8	1113	Sand/Silt - End of Erskine	300 Second Count
255-260	249.0	2.6	14.0	35.6	1114	Clay/Silt - Start of Blina	300 Second Count
260-265	236.4	2.8	13.0	33.0	1115	Clay/Silt	300 Second Count
265-270	236.5	2.6	13.7	32.5	1116	Clay/Silt	300 Second Count
270-275	236.7	2.6	12.6	34.7	1117	Clay/Silt	300 Second Count

APPENDIX F: SCINTILLOMETER READINGS

Table 1. Scintillometer measurements taken at Erskine Point

Interval (m)	Peak Count (cps SPP)	Unit
0-1 (106 m a.s.l)	240	Blina Shale
1-2	180	Blina Shale
2-3	236	Blina Shale
3-4	230	Blina Shale
4-5	253	Contact area/ Blina Shale
5-5.5	264	Contact boundary – sandy layer below
5.5-6	206	Contact boundary – sandy oxidised unit above
6-7	131	Erskine
7-8	136	Erskine
8-9	129	Erskine
9-10 (115 m a.s.l)	123	Erskine